

POLITECNICO DI TORINO

Master's Degree in Mechatronic Engineering



Master's Degree Thesis

**Development of a Payload Dispenser
for Lunar Exploration Rovers**

Supervisors:

Prof. Marcello **Chiaberge**
Dott. Giacomo **Franchini**

Candidate:

Daniele **Genovese**

October 2024

Development of a Payload Dispenser for Lunar Exploration Rovers

Daniele Genovese

October 16, 2024

”Whatever you do in this life,
it’s not legendary,
unless your friends are there to see it”
Barney Stinson

Abstract

Since its beginning, the exploration of planets, moons, and asteroids has been crucial in humankind's development, introducing innovations that have profoundly impacted science, technology, society, and everyday life. This thesis project aims to design, prototype, and test a payload dispenser integrated with lunar exploration rovers. This system must address the unique challenges posed by the extreme lunar environment while deploying a wide range of payloads, such as scientific instruments and localization tags which will enhance the flexibility of lunar missions.

The proposed solution includes the mechanical design of different mechanisms and subsequent analyses of these options to highlight the strengths and weaknesses of each projected subsystem. Moreover, the design of a reliable control logic that autonomously manages the release of each payload has been developed. In order to facilitate the actuators' low-level control logic MicroROS has been adopted. This advanced framework represents the major innovation of this work, allowing the execution of a ROS2 node directly on microcontrollers. Furthermore, using cameras in combination with gyroscopes and accelerometers, a feedback system has been designed to evaluate the pose of the deployed payloads and their position relative to the rover and then on the global map. The developed prototype underwent both computer simulations and physical testing to verify the structural integrity and the actual mechanism performances.

In conclusion, this work introduces an innovative system that contributes to making more versatile, flexible, and autonomous future lunar robotic missions, expanding the available technologies exploitable for space exploration.

Contents

1	Introduction	1
1.1	Current Trends in Planetary Exploration	1
1.1.1	Satellite missions	1
1.1.2	On surface missions	2
1.2	Objective of the Thesis	4
1.2.1	Need for a Rover to Be Capable of Deploying Objects	4
1.2.2	European Moon Rover System (EMRS)	5
1.2.3	Introduction to the Payload sDispenser	5
1.2.4	Objectives of the Payload Dispenser	6
1.2.5	A first type of Payload	6
1.3	Review of Existing Solutions	7
1.3.1	In Orbit Deployments	8
1.3.2	On Surface Deployments	8
1.3.3	On Earth Applications	10
2	Requirements	11
2.1	Lunar Environmental Challenges	11
2.1.1	Vacuum Environment	11
2.1.2	Temperature Extremes	12
2.1.3	Lunar Dust (Regolith)	13
2.1.4	Radiation Exposure	14
2.1.5	Communication Latency and Line-of-Sight	14
2.2	Specifications of the Payload Dispenser	15
2.2.1	Mass Requirement	15
2.2.2	Mechanical interfaces	15
2.2.3	Electrical Interfaces	16
2.2.4	Data interfaces	16
3	Mechanical Design	17
3.1	Selection of Technologies and Materials	17
3.2	Description of Considered Design Alternatives	19
3.2.1	Opening Mechanisms	20
3.2.2	Release mechanisms	24
3.3	Comparison and Selection of Design Alternatives	25
3.3.1	Opening Mechanism Selection	25
3.3.2	Release Mechanism Selection	27

3.4	Presentation of Structural Components	30
3.4.1	Duct and its Support	30
3.4.2	Spacer Ring	31
3.5	Selected Mechansims analysis	32
3.5.1	Shutter CAD models	32
3.5.2	Release Arm CAD models	37
3.6	Simulations and Structural Analysis	39
3.6.1	Analysis of the Forces Involved	39
3.6.2	Simulation Results	41
4	Electronic and Control Design	45
4.1	General Architecture	45
4.1.1	Integration with the Lunar Rover	45
4.1.2	Rover Payload Central Computer	45
4.1.3	Microcontroller	46
4.1.4	Signal Decoupler	47
4.1.5	Actuators	48
4.2	Control Logic	49
4.3	Payload Feedback Mechanism	51
4.3.1	Active Feedback	51
4.3.2	Passive Feedback	52
4.4	MicroROS and its integration in the project	55
4.4.1	MicroROS's Advantages	55
4.4.2	MicroROS integration in the project	55
4.5	An Overview on the Software Architecture.	56
4.6	Components testing	56
4.6.1	Signal Decoupler testing	57
4.6.2	AprilTag testing	60
4.6.3	MPU and Madgwick Filter testing	63
5	Realization of the Prototype	65
5.1	Production Process	65
5.1.1	3D Printing Preparation Steps	65
5.1.2	3D Printed Components	66
5.2	Assembly Process	67

6	Testing Phase	71
6.0.1	Test Setup	71
6.0.2	Test Results	73
7	Conclusion	75
7.1	Project summary	75
7.2	Summary of Achieved Results	75
7.3	Contributions to Innovation of the Project	76
8	Future Developments	77
8.1	Potential Improvements and Optimizations	77
8.1.1	Deployment Surface Analysis	77
8.1.2	Material Improvements	77
8.1.3	Release Mechanism	78
8.2	Applicability in Other Contexts	79
8.2.1	Celestial Bodies Exploration	79
8.2.2	Support for Extravehicular Missions	79
8.2.3	Exploration of Extreme Terrestrial Environments	80
8.2.4	Urban deliveries	80
9	Appendix	81
9.1	Guide to MicroRos Usage	81
9.1.1	Prerequisites	81
9.1.2	PlatformIO Setup	81
9.1.3	MicroROS agent	86

List of Figures

1	The Cassini spacecraft passes between Saturn and its rings. [1]	1
2	Philae touchdown on comet 67P. [2]	1
3	Natural and False Color Views of Europa. [4]	2
4	Curiosity rover. [6]	3
5	In orbit deployment of the DUSTEE spheres. [7]	3
6	UWB anchors network. [8]	4
7	EMRS rover and its subsystems.	5
8	UWB Anchor Prototype. [9]	7
9	Artist Concept of LSMS Unloading Lander. [12]	9
10	CAD model of LPDS mounted on rover. [13]	9
11	UGV unit carrying an APDS. [14]	10
12	Plato Crater and Sinus Iridum on the Moon. [15]	11
13	Moon's Surface Temperature. [16]	12
14	Moon Dust Micrographs. [20]	13
15	On the left, the Trapdoor Mechanism closed. On the right, the same mechanism opened.	20
16	On the left, the Iris Mechanism opened. On the right, the same mechanism closed.	22
17	On the left, a view of the Iris mechanism with a transparent upper plate. On the right, a view of a flap.	23
18	On the left, the Shutter mechanism opened. On the right, the shutter mechanism closed.	24
19	A view of the Shutter mechanism with a transparent upper plate.	25
20	On the left, the front view of a flap. On the right, the back view of a flap.	26
21	A view of a duct equipped with the Release Arm.	27
22	On the left, a zoomed-in view of the contact between the central duct and the payload, which holds the probe in place. On the right, the same setup viewed from below.	28
23	On the left, a side view of the system in release position. On the right, the same setup viewed from below.	28
24	CAD views of the Duct Structure.	31
25	CAD views of the Guide Ring.	31
26	CAD view of the exploded Shutter.	32
27	CAD view of the Shutter's base.	33

28	CAD views of the Guide Ring.	34
29	CAD views of a Flap.	34
30	CAD view of a rod.	35
31	CAD views of the Guide Ring.	35
32	CAD view of a Spring Plugger's support.	36
33	RS PRO's Spring Plugger. [22]	36
34	CAD view of the exploded Release Arm mechanism.	37
35	CAD view of the Actuator Arm.	37
36	CAD views of the Motor Support.	38
37	CAD views of the Motor Support.	38
38	The placement of the fourth Payload, for simplicity two of three ducts has been removed.	39
39	Shutter's yielding graph.	41
40	Shutter's displacement graph.	41
41	Shutter's coefficient of security graph.	42
42	Shutter's yielding graph.	43
43	Shutter's displacement graph.	43
44	Shutter's coefficient of security graph.	44
45	RPi5's schematic top view.	46
46	ESP32 DevKit V1's schematic top view.	47
47	Decoupling circuit's schematic view.	48
48	MicroServo 9g.	48
49	PWM signal and related servo position. [23]	49
50	Control logic diagram.	50
51	Inside view of the validation payload.	52
52	Top view of a payload equipped with AprilTag.	53
53	The cam, that is used for AprilTag detection, placed on the bottom of the payload dispenser.	54
54	RQT_graph of ROS2 environment.	56
55	The Decoupling Circuit implemented on a breadboard.	58
56	Oscilloscope signal visualization. In yellow, the input waves; in light blue, the output ones.	59
57	ID0 25h9 AprilTag.	60
58	AprilTag Distance Testing Setup.	61
59	On the left, the BambuLAB A1 mini used to print the com- ponents. On the right, the preparation plate of the Duct.	65
60	BambuLabA1 during the printing process of the Release Arm.	66
61	Disassembled Payload Dispenser.	67

62	Figures (a) shows the Base and the Guide Ring mounted on the panel. In Figure (b) the a Rod that links the Guide Ring and a Flap. In Figure (c) the Rotating Cover. In Figure (d) the Spring Plugger.	68
63	Figures (a) shows the Spacer Ring fixed on the panel. In Figure (b) the a Rod that links the Guide Ring and a Flap. In Figure (c) a top view of the system.	69
64	The mechanism that actuates the Rotating Plate.	70
65	Payload Dispenser mounted on the testing chassis.	71
66	The Payload Dispenser mounted on the chassis.	72
67	RVIZ2 visualization of the released payload and the system. .	73
68	Low Voltage Scanning Electron Microscopy (LVSEM) images of silica aerogel samples. (a) Pristine, uncoated. (b-d) Sputter coated with 5 nm, 16 nm, 32 nm thick Au layers, respectively. [26]	78
69	Piezoelectric schematic working principle. [27]	79
70	Extensions submenu	82
71	PlatformIO installation	82
72	PlatformIO submenu	83
73	PlatformIO project configuration	83
74	Platformio.ini file	84
75	Compilation button	84
76	Correct compilation output	85
77	Upload button	85
78	Correct upload output	85
79	Common error	86
80	Agent starting output	87
81	Agent final output	88
82	Application output	88

List of Tables

1	A6061 Aluminium alloy composition by mass. [21]	19
2	A6061 Generic Physical Properties. [21]	19
3	A6061 Mechanical Properties. [21]	19
4	Qualitative Comparison of Opening Mechanisms Based on Re- quirements.	27
5	Qualitative Comparison of Release Mechanisms Based on Re- quirements.	29
6	AprilTag Size and Measured Coordinates.	62
7	Measurement Average Error.	62
8	Comparison between imposed angles and measured ones. . . .	64

1 Introduction

1.1 Current Trends in Planetary Exploration

Space exploration plays a fundamental role in human evolution. Exploring and studying extraterrestrial environments is extremely significant because it expands our knowledge of the universe, enhances the possibility of finding water and life beyond the Earth, and stimulates technological innovation. Nowadays, not considering the Apollo missions at the end of the 20th century, satellites, rovers, and landers are used to study celestial bodies directly. A remarkable example of satellite missions is represented by the Mars Reconnaissance Orbiter, the Cassini mission, and the Lunar Reconnaissance Orbiter. On the other hand, some noticeable landers and rover missions include the Viking 1 and 2 lander missions, the Curiosity rover, and the Philae lander.

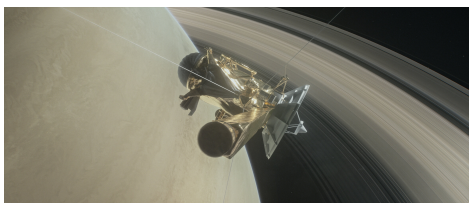


Figure 1: The Cassini spacecraft passes between Saturn and its rings. [1]



Figure 2: Philae touchdown on comet 67P. [2]

1.1.1 Satellite missions

Missions that involve satellites orbiting celestial bodies significantly contribute to increasing the knowledge about planets' and moons' nature. Satellites, thanks to their instrumentation, conduct studies about the atmosphere and the surface of these celestial bodies to get information about their composition and climatic dynamics. Another objective for this kind of mission is the seeking of natural sources that are crucial to reveal potential for life and support for future colonization and exploration missions.

A suitable example of this type of mission is NASA's project Europa Clipper (EC). This satellite has been designed to study Europa, one of the moons

of Jupiter. Europa has gained great interest in recent years because it has shown the potential for a subsurface ocean. The EC, thanks to its advanced instrumentation, will investigate Europa's surface, atmosphere, and ice, to prove the existence of liquid water on this moon. [3]

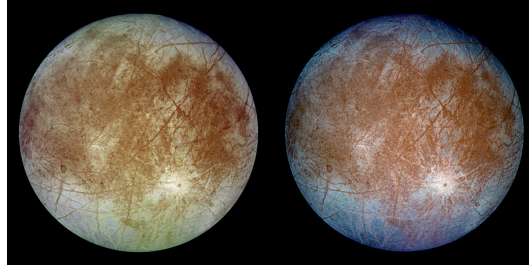


Figure 3: Natural and False Color Views of Europa. [4]

1.1.2 On surface missions

The missions that have as an objective a more detailed analysis of celestial bodies' surfaces use rovers and landers to conduct these studies.

In-depth studying the soil of moons, planets, and asteroids plays a key role in the expansion of knowledge on their formation and evolution. Orbital missions and remote observation cannot offer the same level of detail given by in situ analysis.

Moreover, this kind of mission, directly analyzing rocks, soil, and dust, is fundamental to the search for extraterrestrial life. Additionally, these missions provide crucial information about the presence of natural resources such as water or in-situ building materials. The confirmation of the presence of these materials would be of fundamental importance for the planning of future missions with humans.

Curiosity rover is one of the most famous NASA rover missions. The objective of this rover was to explore Mars's surface and collect information about the rocks and soil composition in ancient riverbeds and clay-rich areas. The analyses conducted by Curiosity helped scientists to understand the planet's geological history and its potential to have hosted life. This rover demonstrates the importance of surface missions to gain more detailed knowledge about the planet's evolutionary story and assess the potential for life beyond Earth. [5]



Figure 4: Curiosity rover. [6]

There are other missions that integrate both the benefits of satellites and surface exploration. A perfect example that combines these two typologies of approach is represented by the deployment of DUSTEE spheres. This sphere has been tailored and designed to investigate the presence of mineral water at the lunar South Pole. The need to in orbit deploy these spheres comes from the fact that the South Pole of the Moon is difficult to be reached by conventional rovers. To avoid a complete surface mission, with the related extreme challenges, the DUSTEE spheres are released in orbit by a conventional CubeSat deployer. Thanks to the orbital release these spheres are capable of covering a wide area of hostile environment, opening new possibilities for research and resource discovery.



Figure 5: In orbit deployment of the DUSTEE spheres. [7]

1.2 Objective of the Thesis

This thesis project aims to develop a prototype system capable of deploying different kinds of payloads on the surface of the Moon. The design of this system must take into account the specific challenges coming from the harsh lunar environment while combining structural simplicity and operational reliability.

1.2.1 Need for a Rover to Be Capable of Deploying Objects

During an extraterrestrial mission, the ability of a rover to deploy payloads such as probes or localization tags is fundamental to enhancing the flexibility and operability of the rover itself.

Indeed, releasing probes in a different zone of interest is the key to analyzing these areas while the rover continues to operate in other sites. These probes can autonomously collect long-term data, such as changes in soil composition or atmospherical variation even beyond the rover's lifespan. This information allows to scientific team to observe the evolutions of conditions of different locations on planets, moons, or asteroids

Another example of items that can be deployed from the rover are UWB anchors. These anchors are fundamental for navigation in complex terrains where direct line-of-sight communication may be difficult.

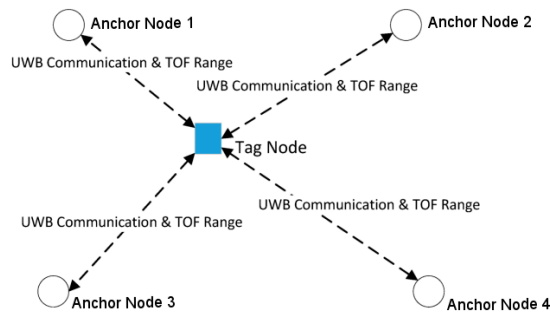


Figure 6: UWB anchors network. [8]

1.2.2 European Moon Rover System (EMRS)

The thesis project fits into the growing trend of developing rovers capable of hosting different types of modular systems. This trend comes from the necessity of enhancing the flexibility of the rover system both during the testing and operational phases. Specifically, a rover that can be referred to is the EMRS. This rover has been developed by Thales Alenia Space Italy to explore the polar regions of the moon. The innovation introduced by EMRS is represented by its structure that offers a common platform capable of hosting different types of systems. These systems range from object manipulation to regolith excavation. A working prototype is already available from 2023, this experimental system has an advanced locomotion mechanism and supports different scientific and engineering payloads.

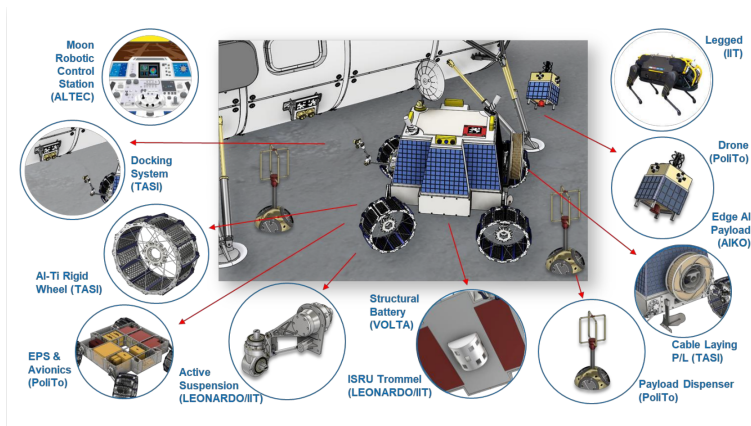


Figure 7: EMRS rover and its subsystems.

1.2.3 Introduction to the Payload sDispenser

The payload dispenser system will be projected to accomplish the task of deploying scientific and technological instruments on the surface of the Moon. Since there are no standardized forms of payloads that may require deployment during an extraterrestrial mission, the payload system must ensure flexibility and adaptability to handle a wide range of payload forms and sizes. A flexible system ensures the operability of the payload dispenser itself in different operational conditions. The system must also guarantee simplicity,

efficiency, and robustness in the harsh lunar environment.

The main goal of the payload dispenser project is to develop a prototype capable of autonomously releasing payloads across the lunar surface and receiving feedback to monitor the deployment. Additionally, to ensure the functionality of the system under mission-like conditions, extensive simulation and testing will be carried out.

1.2.4 Objectives of the Payload Dispenser

The principal goals that the payload dispenser must meet can be summarized as follows:

1. **Design and Prototype Development:** The final objective is to develop a prototype capable of autonomously deploying different types of payloads. The design of this system must be focused on simplicity, efficiency and reliability
2. **Autonomous Operations:** The dispenser must enable the release basing the operation on the commands coming from the rover's central computer.
3. **Data Collection and Analysis:** The prototype must collect data about the release system to define the performance, positioning accuracy, and potential benefits of the payload dispenser.

1.2.5 A first type of Payload

During the design and testing phase a payload consisting of a sphere containing a UWB anchor is considered. This anchor perfectly represents the type of payload that will be used in correlation with the Payload Dispenser because the sphere can be easily redesigned to accommodate other types of scientific instruments. For this reason, the entire project is based on the dimension of this UWB anchor, which was designed by Michelangelo Levati during his master's thesis project. [9]

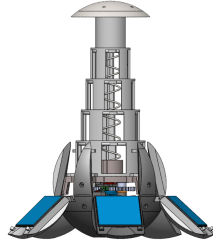


Figure 8: UWB Anchor Prototype. [9]

1.3 Review of Existing Solutions

During the design and development of the payload dispenser, looking at existing solutions is crucial to obtain a well-structured system. In this section, a review of current payload dispenser systems and related technologies used both in space exploration and other applications is presented.

This review goes through an overview of payload dispensers, technological innovations, and challenges faced by pre-existing systems. The insights gathered from examining these previous solutions will lead to the development of a more effective and tailored system for lunar missions.

However, it is important to highlight that, for the specific case of a payload dispenser designed for a surface lunar mission, no fully developed systems currently exist. Even if there are various types of payload dispensers, the absence of a directly comparable system necessitates a careful adaptation of existing technologies to meet the specific requirements set by the lunar environment.

The insights gained from reviewing existing solutions will be the key to bridging this gap, guiding the design and innovation necessary to develop a payload dispenser capable of operating under harsh lunar conditions.

1.3.1 In Orbit Deployments

When an object is released into the orbit of a planet or moon, it can either remain in orbit or descend to the surface. The first situation is typically represented by satellites, which are usually deployed using CubeSat deployers or Canisterized Satellite Dispenser (CSD) (a more advanced form of CubeSat deployer). On the other hand, the second situation is more unusual. An example is the previously mentioned deployment of DUSTEE spheres.

- **CubeSat:** CubeSats are small, standardized satellites designed for space missions. They are characterized by their modular and compact design. Each unit, also called "U", measures 10x10x10 cm with a mass of about 1.33 Kg. These satellites are released as secondary payloads from larger rockets, making them a cost-effective option for space exploration and experimentation. Thanks to their modular design it is easier to integrate and deploy them in more complex systems enabling a wide range of missions. [10]
- **Canisterized Satellite Dispenser:** It is a device used to deploy multiple small satellites from a single launch vehicle. A typical example of satellites deployed by this system is the already cited CubeSat. The CSD holds the satellites in a cylindrical duct and releases them into space in a controlled manner. The deployment occurs by opening the canister and ejecting the satellites at precise intervals. This system enables efficient and organized deployment, allowing the simultaneous launch of several small satellites. [11]

1.3.2 On Surface Deployments

In the case of on-surface deployments, two distinct scenarios can be distinguished:

- **Weighed Payloads:** When the challenges involved in constructing a lunar outpost are analyzed, the movement of the different prefabricated components will be crucial to complete the construction of a lunar base. A prototype system, that is a perfect example for this purpose, is the Lunar Surface Manipulation System (LSMS). This device is capable of lifting and handling heavy payloads on the lunar surface. Its operational goal is to support key operations such as unloading landers, precisely positioning components and preparing the outpost's site by

excavating regolith. Its versatility and adaptability make it essential for efficiently moving and assembling the large components necessary for establishing a functional lunar outpost. [12]



Figure 9: Artist Concept of LSMS Unloading Lander. [12]

- **Ligh Weight Payloads:** When there is a need to deploy items, such as probes or relays, the typical solution is to use a deployment system carried by a rover. This solution has been sketched by a Lockheed Martin team that has developed a first prototype of a deployer. A perfect example is the Lunar Payload Deployment System (LPDS) designed by a Lockheed Martin's team for NASA's Artemis program. The LPDS is designed to be integrated into lunar rovers, enabling the deployment and movement of light payloads on the lunar surface. This system includes components such as a grappling mechanism, a vertical actuator and sensors for autonomous operations. All these elements are tailored to withstand the harsh lunar conditions. the first prototype, built with 70% mass reduction, shows how such system can effectively deploy small payloads essential for a lunar mission. [13]

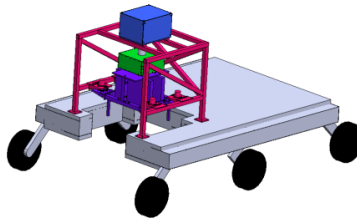


Figure 10: CAD model of LPDS mounted on rover. [13]

1.3.3 On Earth Applications

Regarding terrestrial applications, the deployment of object finds large application in the maintaining of communication for Unmanned Ground Vehicles (UGV). A notable example is the prototyping of the Automatic Payload Deployment System (ADPS).

The APDS was designed to face the challenges of deploying various types of payloads in harsh or inaccessible environments. Initially, it was inspired by the Autonomous Mobile Communication Relays (ADCR) project, which aimed to maintain communication with UGVs beyond the line of sight. This system, in order to accomplish its goal, uses a convoy of mobile relay nodes, which increases the cost of the total system. Building on the ADCR, the APDS was designed with enhanced capabilities, allowing it to deploy a wide range of payloads, not only relay bricks. This system includes a deployer that can communicate with the central computer and release various types of payloads, such as cameras, infrared illuminators and other devices. The flexibility of the APDS enables UGVs, that use this system, to autonomously perform tasks such as maintaining communication in challenging environments or supporting rescue missions. [14]



Figure 11: UGV unit carrying an APDS. [14]

2 Requirements

In this chapter, the main challenges that a rover, and generally any system, must face to operate under the lunar environment will first be highlighted. Then, the technical specifications that the payload dispenser must meet to ensure the success of the mission will be analyzed in detail.

2.1 Lunar Environmental Challenges

The Lunar surface is characterized by a unique set of challenges for each type of mission, especially for systems like rovers and landers that have different critical moveable components. In contrast to the Earth's environment, the Moon has an extreme and harsh environment. Indeed, the lunar surface is characterized by vacuum, severe temperature fluctuations, abrasive dust, and high radiation levels. Each of these aspects has a notable impact on the design, operation, and durability of the rover and its subsystems, such as the payload dispenser. This section studies the most relevant environmental challenges and their impacts on the payload dispenser development.



Figure 12: Plato Crater and Sinus Iridum on the Moon. [15]

2.1.1 Vacuum Environment

In a vacuum, traditional lubricants can evaporate or degrade, leading to increased wear and potential failure of mechanical components. The payload dispenser's moving parts, such as motors or gears must use vacuum-compatible lubricants or rely on solid lubrication techniques, such as using materials like graphite or molybdenum disulfide, to ensure smooth operation.

2.1.2 Temperature Extremes

The temperature on the moon's surface varies greatly during the lunar day. Indeed, during the lunar night, the temperature of the satellite's surface drops to -180°C from about $+120^{\circ}\text{C}$ while exposed to the sun. The temperature shift poses a significant challenge to the rover's and its subsystems' thermal management.

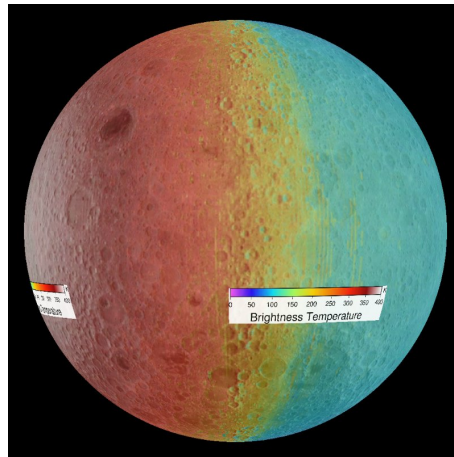


Figure 13: Moon's Surface Temperature. [16]

- **Thermal Expansion and contraction:** It is crucial that all components subjected to drastic temperature fluctuations are designed to effectively face thermal expansion and contraction while maintaining structural integrity. Selecting materials with similar coefficients of heat expansion and designing the components with thermal resilience is essential to addressing this problem. The secret to preventing mechanical stress or misalignment is to follow these precautions.
- **Thermal Insulation:** To protect sensitive electronics and mechanisms from high temperatures, well-structured thermal insulation is necessary. Multi-layer insulation and thermal coatings help to minimize heat exchange. On the other hand, the internal heater may be required to maintain operational temperature during the lunar night.
- **Thermal Management:** Since the lunar has not an atmosphere, heat dissipation must rely on radiation and conduction. Efficient heat man-

agement is essential. In particular, overheating must be avoided for active components, such as motors and electronics.

2.1.3 Lunar Dust (Regolith)

Lunar dust, also called regolith, represents another remarkable challenge due to its abrasive and adhesive properties. The fine particles of lunar dust can penetrate inside the mechanical systems and cause performance degradation or malfunctions.

- **Abrasiveness:** Moon sand has sharp edges [17] that, accumulating, can wear out the moving components inside the mechanisms. The selection of abrasion-resistant materials is the key to the longevity of the whole system.
- **Dust Mitigation:** Seals, barriers, and specialized surface treatments are required to protect critical components from regolith infiltrations.
- **Static Charge and Adhesion:** The lunar dust can be electrically charged by solar radiation. This phenomenon leads to an increase in its adhesion to surface property. [18] [19]. Implementing electrostatic discharge protection for the relevant electronics and exposed areas can reduce the risk of interference.

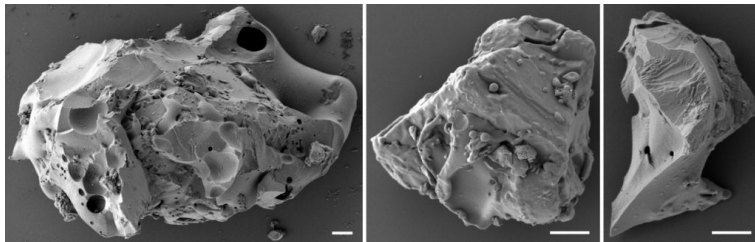


Figure 14: Moon Dust Micrographs. [20]

2.1.4 Radiation Exposure

The Moon does not have neither a magnetic field nor an atmosphere. This leaves the Moon's surface exposed to high level of radiation and solar particle events. This radiations can affect the electronic inside systems and degrade materials, influencing the life and the operational reliability of the whole system.

- **Radiation Hardened Components:** The usage of radiation hardened components is essential to face a long exposure to cosmic rays and solar radiations. To ensure the continued functionality of electronics, the utilization of radiation tolerant microprocessors, memory devices and power system is necessary.
- **Shielding:** Even if, due to weight limitations, a complete radiation shielding may not be possible, localized shielding around sensitive components is for sure required. Components like aluminium or specialized composites offer a partial protection against radiations.

2.1.5 Communication Latency and Line-of-Sight

The Moon is hundreds of thousands of kilometers away from Earth, this leads to a communication delay of approximately 1.3 seconds each way, complicating the real time control. To face the problem related to this latency, the rover and its subsystems must operate autonomously in the majority of the situation.

- **Autonomous Operations:** The capability of executing autonomous actions, based on a pre-programmed sequences and decision making algorithm running on the rover central computer, is crucial for the functionality of each rover's subsystem. This capability allows to the rover to perform its tasks efficiently despite the communication delays.
- **Loss of Line-of-Sight:** Since the lunar surface terrain is extremely uneven, the rover may experience temporary loss of communication with the lander/Earth. For this reason, it is essential for the rover to store and execute commands and data during these periods. Continuing operations even during loss of signal is essential for the success of the mission.

In conclusion, the lunar surface presents a high number of challenges that must be considered during the design of a rover and its subsystems. Each condition imposes constraints that impact the choice of materials, mechanical design and electrical architecture. By anticipating and considering these issues, the subsystems and in this case the payload dispenser can maintain reliable performances in the lunar environment throughout the entire mission. In this thesis project, since the final goal is to realize a basic prototype of a payload dispenser, some of these factors will be considered that will guide the whole design process.

2.2 Specifications of the Payload Dispenser

In this section, a detailed overview of the requirements and interfaces for the payload dispenser is provided. These specifications are required to ensure an optimal integration with rovers mechanical, electrical and data subsystems. Given the operational environment and the cost to send a rover to the Moon's surface, the dispenser must meet strict constraints for mass, mechanical interfaces and communication protocols.

2.2.1 Mass Requirement

Keeping the mass to its minimum is crucial due to its impact on the rover's mobility, balance and energy consumption. Furthermore, the greater the mass, the greater the mission costs. A lighter dispenser contributes to improve the rover performance, enhancing the energy usage and reducing the stress on the vehicle.

2.2.2 Mechanical interfaces

A well structured mechanical integration between the payload dispenser and the rover is critical to ensuring a modular and adaptable design. The dispenser must be designed with a modular form factor, in order to allow an easy attachment, detachment and potential reconfiguration. The modularity has a key role to improve the flexibility of this subsystem, enabling quick changes or replacement during the testing phase of the whole rover system. The modularization also supports future upgrades or variations in payload types without necessitating major redesigns.

2.2.3 Electrical Interfaces

In order to correctly work, the payload dispenser requires a reliable power and data connections with the rover's electrical architecture. The dispenser does not necessarily work with specific voltages but must be compatible with the voltages typically used inside the rovers.

Usually, rovers provides power att 5V, 12V and 24V. The payload dispenser must be designed to draw power from one or more of these available source. The selection of which voltage to use will depend on the specific power requirements of the dispenser internal subsystems.

2.2.4 Data interfaces

The data communication between the dispenser and the rover's central computer is managed by USB interface. This ensures standardization of the communication and reliability. The protocol chosen to communicate via USB is MicroROS, which will handle the data exchange.

3 Mechanical Design

An accurate mechanical design phase is the first step to produce a reliable system. During this phase, the constraints analyzed before are translated into practical engineering decisions. The final prototype obtained through the design process must ensure a system that meets both the functional requirements and the environmental constraints posed by the extreme lunar environment. During the design process, each component is designed with attention to simplicity, robustness, reliability, and flexibility and considering, at the same time, the unique operational conditions posed by the Moon. Considering all these factors, the prototype will not only meet the mission objectives but will also demonstrate resilience and efficiency in addressing the mentioned challenges.

3.1 Selection of Technologies and Materials

The initial stage of the mechanical design is represented by the selection of materials and technologies that will be used for the final prototype or for the computer simulations. An accurate choice of materials is crucial to ensure that the system is able to withstand the harsh lunar environment. Indeed, materials are one of the most relevant factors that impact system's performance and reliability. However, given that the aim of the thesis project is the development of a prototype, some decisions will be guided by practical constraints such as costs and the availability of materials and components. The chosen material will be used to carry out the FEM analysis to obtain a reliable structural integrity simulation. However, the prototype will mainly consist of components printed in PLA being a material suitable for the first phase of system realization to validate its functionality.

Criteria for Material Selection

Different crucial criteria must be taken into account when choosing materials for a lunar system. However, it is important to remember that the mission-grade design will require further refinements.

- **Vacuum Compatibility:** Prototypes with a higher level of development could be tested in conditions near to the lunar environment. The vacuum represents one of these conditions. In this case, material

selection must prefer low-outgassing materials. Nevertheless, at this stage of prototyping, vacuum is not considered in order to adopt more accessible and cost-effective alternatives.

- **Thermal Stability:** Due to extreme temperature variations, the simulated components must demonstrate resilience to thermal dilatation and contraction. For this reason, a material with a reasonable thermal coefficient will be selected.
- **Abrasion Resistance:** Given the presence of highly abrasive lunar dust, the material chosen must prove resistant to abrasion.

Final Selection of Materials

Considering the goal of the mission, the following material has been selected. For aerospace applications, aluminum alloys of the 6000 series are typically used. In this case, the A6061 is ideal for this application. Thanks to its properties, this aluminum alloy is widely used in the aerospace and engineering fields. Below are mentioned the major benefits that make the A6061 particularly advantageous for the design of the payload dispenser.

This alloy is known for its excellent strength-to-weight ratio. Thanks to these properties, A6061 allows to design of light components capable of tolerating significant stress. This factor is crucial for aerospace applications that typically involve stringent requirements on the mass of components.

Additionally, the A6061 has an optimal resistance to corrosion. This property is of great importance when components are exposed to harsh environments, such as the lunar surface. Hence, using this alloy it is possible to extend the lifespan of systems, making them suitable for long-term missions.

Furthermore, the A6061 is easily workable. This is very important to be able to create custom-made pieces.

Moreover, this aluminum alloy provides a suitable thermal conductivity. This feature helps to manage heat dissipation maintaining the performance reliable under extreme temperature variation.

Finally, the A6061 is known for its very good weldability. The components can be joined using standard welding techniques. This represents a great advantage when there is the necessity to assemble complex structures in a robust way.

It is important to remark that the final system will use prototyping materials detailed in the following chapters.

Constituent element	Minimum (% by weight)	Maximum (% by weight)
Al	95.85%	98.56%
Mg	0.80%	1.20%
Si	0.40%	0.80%
Fe	0	0.70%
Cu	0.15%	0.40%
Cr	0.04%	0.35%
Zn	0	0.25%
Ti	0	0.15%
Mn	0	0.15%
(others)	0	0.%

Table 1: A6061 Aluminium alloy composition by mass. [21]

Property	Value
Density	2.70 g/cm ³
Melting Point	650 °C
Thermal Expansion	23.4 × 10 ⁻⁶ /K
Modulus of Elasticity	70 GPa
Thermal Conductivity	166 W/m · K
Electrical Resistivity	0.040 × 10 ⁻⁶ Ω · m

Table 2: A6061 Generic Physical Properties. [21]

Property	Value
Proof Stress	240 Min MPa
Tensile Strength	260 Min MPa
Hardness Brinell	95 HB

Table 3: A6061 Mechanical Properties. [21]

3.2 Description of Considered Design Alternatives

The development of the payload dispenser requires a careful analysis of the proposal subsystem designs. Each mechanism that composes the dispenser has been chosen among different alternatives. The final choice was determined by the evaluation of each proposal on the basis of the properties that characterize the mechanism.

In general, the chosen mechanism must balance structural simplicity and operational reliability.

3.2.1 Opening Mechanisms

The opening mechanism represents the interface between the interior part of the dispenser and the external world. For this reason, it is crucial to protect the system from the infiltration of lunar dust, which can damage the mechanisms. To address this problem, the opening mechanism must provide a secure seal capable of keeping the dust outside during the movement of the rover. Furthermore, the mass and dimensions of this mechanism, as with all other mechanisms, must be kept to a minimum. Therefore, the mechanism must be compact and light.

1. Trapdoor mechanism

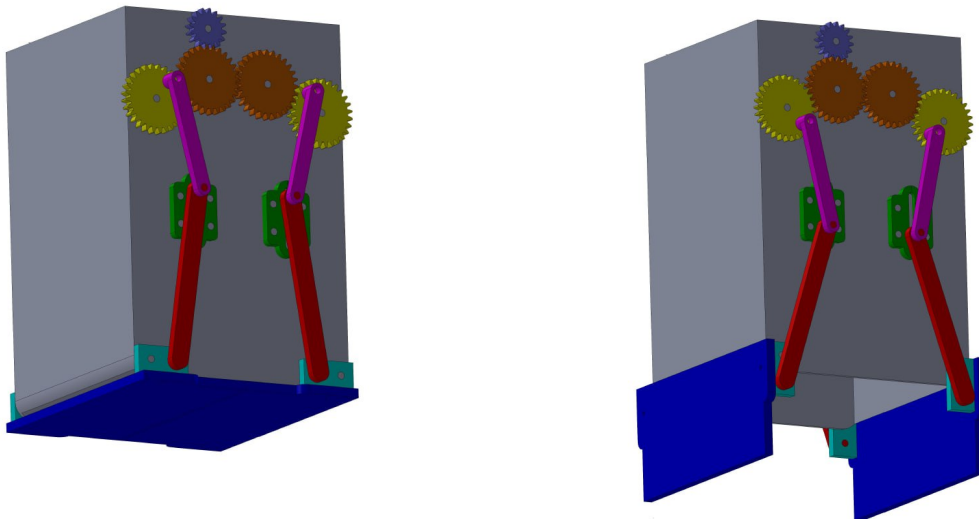


Figure 15: On the left, the Trapdoor Mechanism closed. On the right, the same mechanism opened.

This first mechanism consists of a series of gears that control two articulated arms. These arms are connected to the opening panels, which act as a trapdoor. The gears are driven by a motor. As the gears turn, they move the attached arms, which, in turn, pivot around their connection points. According to the sense of rotation, the motion causes

the trapdoor to open or close. In particular when the pinion (the gear in purple), that is directly attached to the motor, rotates clockwise, the arms push the trapdoor downward, opening it to allow for the deployment of a payload. When the pinion rotates in the opposite direction, the arms pull the trapdoor back into the closed position, securing the contents inside the mechanism and sealing it to prevent the entering of lunar dust. The same type of mechanism can be replicated on the other side of the duct. The mechanism can be replicated either actively (by driving another wheel) to ensure redundancy, or passively.

2. Iris Mechanism

Both this mechanism, called the Iris Mechanism, and the next one are inspired by the diaphragm mechanism of cameras, which are used to regulate the amount of light passing through the lens. Its ability to open and close in a controlled manner makes it an ideal solution for the opening mechanism. This mechanism consists of two plates that rotate relative to each other. The upper plate (the orange one in Figure 19) is the movable plate, while the other one (blue in Figure 20) is fixed to the base of the system. When the upper plates rotate, it causes the flaps (green in Figure 19) to open or close. The flaps have been designed to ensure the sealing of the system when they close and to form a circular shape when it opens allowing the payload to pass through. In Figure 19, a small gap is present at the center of the system. It can be filled with rubber in order to ensure a smoother and more effective closure. It is important to note that the flaps move thanks to the presence of pins, holes and grooves both on the plates and on the flaps themselves. These pins, holes and grooves rigidly guide the movement of the flaps.

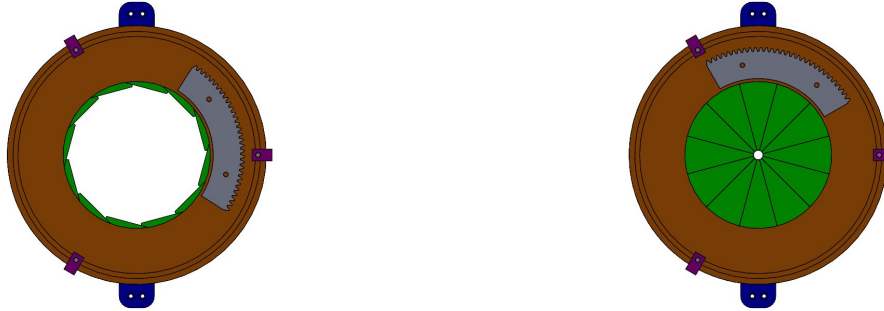


Figure 16: On the left, the Iris Mechanism opened. On the right, the same mechanism closed.

It is important to note that the movement of the flaps is guided by grooves on the surfaces of both plates. Each flap has a groove and a hole that allow them to follow these grooves during the movements.

3. Shutter Mechanism

This last mechanism, also inspired by the diaphragm, works similarly to the previous one. In this case, as well, there are two plates that rotate relative to each other: one is fixed (green in Figure 21), and one is movable (red in the figure 22).

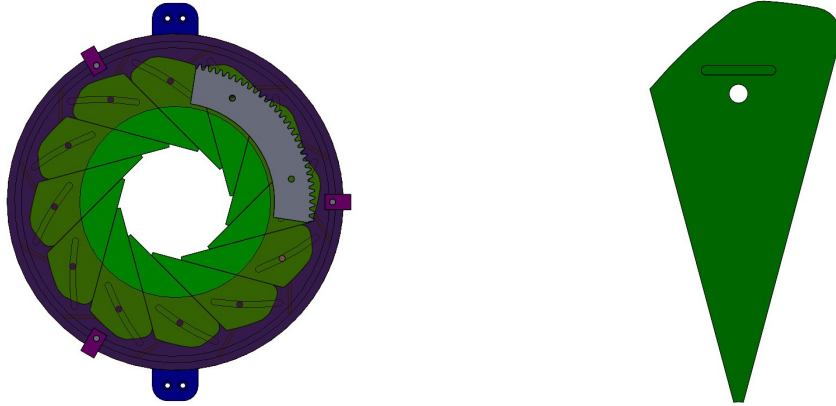


Figure 17: On the left, a view of the Iris mechanism with a transparent upper plate. On the right, a view of a flap.

In contrast to the previous mechanism, in this case, the flaps move thanks to rods (orange in Figure 22) that are connected to a ring (blue in Figure 22) which moves together with the upper plate. When this plate rotates, depending on the sense of rotation, the rods either pull or push the flaps, causing the opening or closing of the system. As in the previous case, the flaps of this system are designed to guarantee both a circular shape when opening and a seal when the system closes.

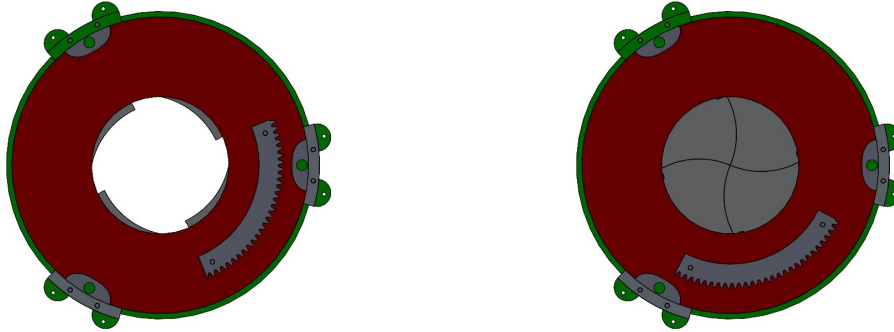


Figure 18: On the left, the Shutter mechanism opened. On the right, the shutter mechanism closed.

3.2.2 Release mechanisms

The second considered subsystem is the release mechanism. This mechanism manages the release of the payload from its location. To obtain a reliable mechanism this must be as simple as possible. In fact, the guiding principle followed in the design of this subsystem was to rely as much as possible on the lunar gravity force to complete the release.

1. Release Arm

The system uses an arm to initially hold the payload in place and then, release when required opening the arm and letting the payloads slides on the inclined base of the duct. The mechanism's strength lies in its simplicity and ease of prototype creation. In fact, creating a small groove on the side of the duct and adding a housing for the servo motor, is enough to achieve a reliable system. Additionally, the arm is easily integrated with the servo motor thanks to the small support already included in servo motor kits. Simply printing an arm with a housing for the support, which will fit onto the servo motor, completes the setup. This straightforward approach ensures that the system is both efficient and accessible.

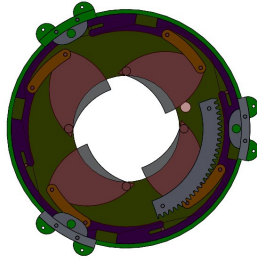


Figure 19: A view of the Shutter mechanism with a transparent upper plate.

2. Selector Mechanism

The second mechanism uses only one stepper motor to select and release the payload to deploy. This motor drives a gear system that, due to the design of a central duct, can lock all the payloads in place and then selectively release a single payload.

3.3 Comparison and Selection of Design Alternatives

After the presentation of the different alternatives for the subsystems of the payload dispenser, it is essential to compare them to select the best alternative that addresses the mission specifications. The main properties that will be used as evaluation criteria in this section are mechanical reliability, ease of manufacturing (both in the prototype and final production phase), adaptability to the lunar environment, minimization of weight and dimensions, and the overall operational complexity.

This comparison will point out the strengths and weaknesses of each alternative. The selected mechanism must offer a balance between performance, reliability, and feasibility. The selected mechanism will be analyzed in more detail in the following sections.

3.3.1 Opening Mechanism Selection

The lunar environment is highly demanding, which is why it is important to carefully choose the opening mechanism to prevent any unwanted interaction

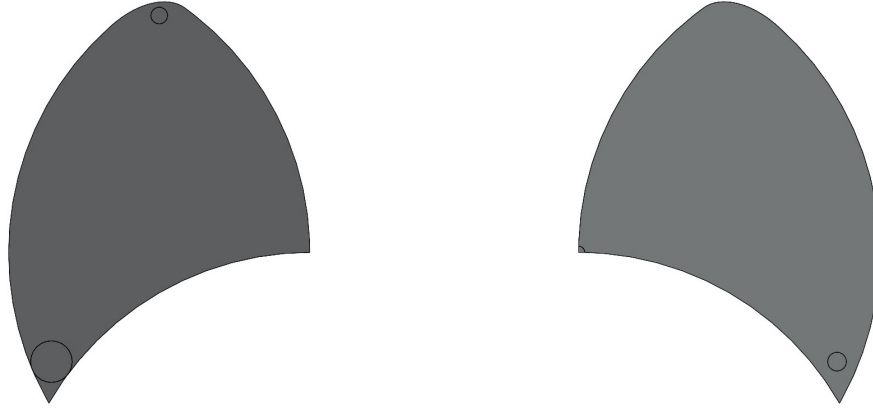


Figure 20: On the left, the front view of a flap. On the right, the back view of a flap.

between the payload dispenser and the outside world. The three proposed mechanisms will be analyzed with particular attention to their ability to combine mechanical reliability, sealing capacity, and operational simplicity. The Trapdoor Mechanism finds its strengths in its simplicity and the possibility of creating a redundant mechanism. Furthermore, this mechanism offers a simple but effective closing mechanism capable of isolating the payload dispenser from the lunar environment. However, the need for additional conduit, required for the installation of the gear mechanism, increases both the mass and the total footprint going against the design specifications.

On the other hand, the Iris Mechanism implements a totally different opening mechanism ensuring a smooth movement during both the opening and the closure. Since this mechanism is based on a radial design, the system is extremely compact. However, a crucial consideration must be made: the mechanism is based on movement along grooves. This can lead to enormous complications due to the thermal expansion to which the components will be subjected. This compromises the reliability of the entire system and therefore cannot be accepted as a solution.

Finally, the Shutter Mechanism, which improves the mechanism seen in the Iris system by using a lower number of components with fewer relative moving parts, offers a more reliable system as it is less subject to thermal expansion. At the same time, this mechanism ensures smooth movement and excellent

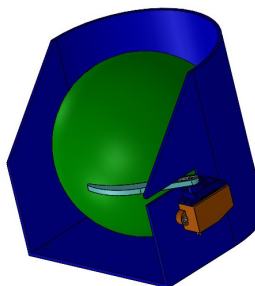


Figure 21: A view of a duct equipped with the Release Arm.

sealing. Although this system is more complex than the Trapdoor Mechanism, it offers an excellent balance of mechanical reliability and functionality. Taking into account the analysis of the various mechanisms, the Shutter is the best compromise. Indeed, it meets all the specifications of the mission while maintaining a relative operational simplicity.

Requirement	Trapdoor Mechanism	Iris Mechanism	Shutter Mechanism
Mechanical Reliability	X	X	X
Sealing Effectiveness	X	X	X
Operational Simplicity	X		X
Size Optimization		X	X
Mass Optimization		X	X
Thermal Expansion Compliance	X		X

Table 4: Qualitative Comparison of Opening Mechanisms Based on Requirements.

3.3.2 Release Mechanism Selection

The choice of the Release Mechanism follows the aforementioned principles of simplicity, reliability, and robustness. At the same time, the system must minimize mass and volume while keeping the number of components to a minimum. Furthermore, the restrictions imposed by the lunar environment must always be considered.

Both proposed solutions will be analyzed to find the one that best meets the

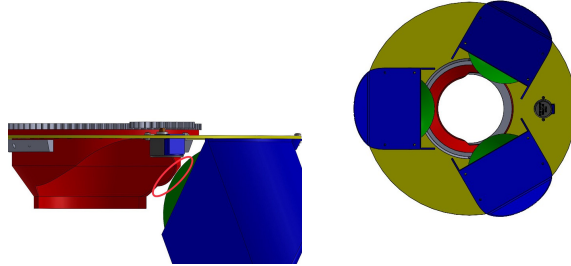


Figure 22: On the left, a zoomed-in view of the contact between the central duct and the payload, which holds the probe in place. On the right, the same setup viewed from below.

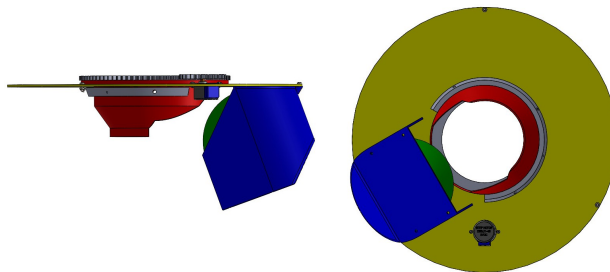


Figure 23: On the left, a side view of the system in release position. On the right, the same setup viewed from below.

requirements while addressing the challenges posed by the mission. The Release Arm stands out for its simplicity, which is its greatest strength. Since there are no relative moving parts, this system responds well to thermal expansion. However, a downside of this solution lies in the fact that it requires a servo motor for each payload. On the other hand, servomotors can not only provide a fairly high torque but at the same time they are reliable and their operations management is basic. The second system, the Selector Mechanism, has been designed following another approach: instead of individually controlling the release of each payload via a servomotor, a stepper motor is used to allow the descent of one payload at a time. This approach allows for reducing the number of active components needed. However, the mechanism that blocks the probes not only requires an articulated shape but also components in relative motion.

This could result in misalignments and interruptions in motion due to thermal expansion. Furthermore, the mechanism weighs down the system and increases the total size compared to the previous one.

In conclusion, although the second mechanism requires fewer actuators, the Release Arm better summarizes the need for a simple, reliable and effective system.

Requirement	Release Arm	Selector Mechanism
Mechanical Reliability	X	X
Minimization of components		X
Operational Simplicity	X	
Size Optimization	X	
Mass Optimization	X	
Thermal Expansion Compliance	X	

Table 5: Qualitative Comparison of Release Mechanisms Based on Requirements.

3.4 Presentation of Structural Components

This section provides an overview of the structural components that are integral to the design and functionality of the project. Although these components are not the primary focus of the system, they are essential for ensuring stability, support and proper integration of the core mechanism.

The design and functionality of each structural component will be examined, demonstrating their role in maintaining the overall integrity and performance of the system.

3.4.1 Duct and its Support

Each payload will be housed within a duct, where it will be held in position and released by the Release Arm. Since the release mechanism relies on gravity to allow the payload to slide toward the hatch, the duct must feature an inclined base to enable passive release. This inclination is provided by an inclined support specifically designed to optimize mass and space. The support is designed to match the duct's shape so that it can be easily attached. The duct has been designed in order to prevent damage to the payload. For this reason, the duct has been developed based on the shape of the modular payload container (basically a sphere), minimizing internal movement and optimizing the dimensions of the duct itself. It is important to take into account that, when the duct is realized for the final system, particular attention must be given to the finishing of the base, where friction between the base and container must be minimized. This precaution comes from the fact that the lunar gravity is one-sixth of Earth's gravity. Additionally, the rear of the duct has an inclined side in order to reduce the overall footprint. On the side of the duct, there is a slot that allows for the operation of the Release Arm. Finally, the top part is equipped with a perforated ring that can be used to secure a cover plate on each individual duct or on the entire system.

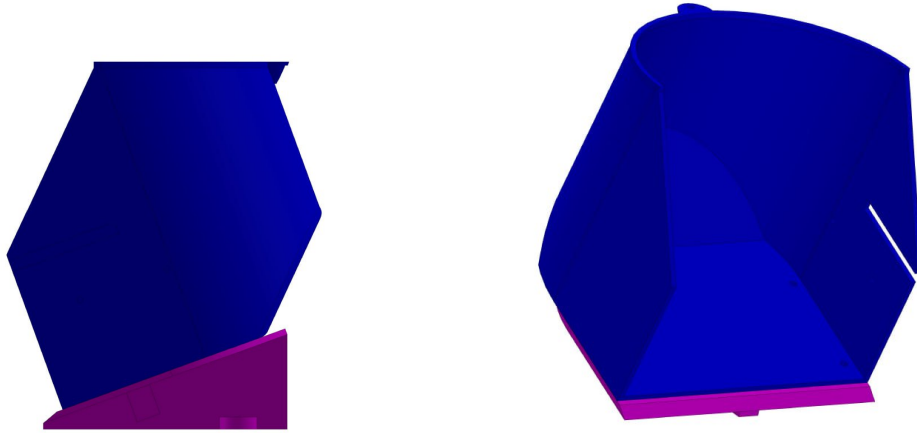


Figure 24: CAD views of the Duct Structure.

3.4.2 Spacer Ring

The Spacer Ring is positioned around the central hole of the base plate, in front of the ends of the ducts. It features grooves corresponding to the ducts that facilitates the sliding of the payload containment modules. Additionally, it has three perforated semicircle around the outer dside to allow for the connection with the base plate.

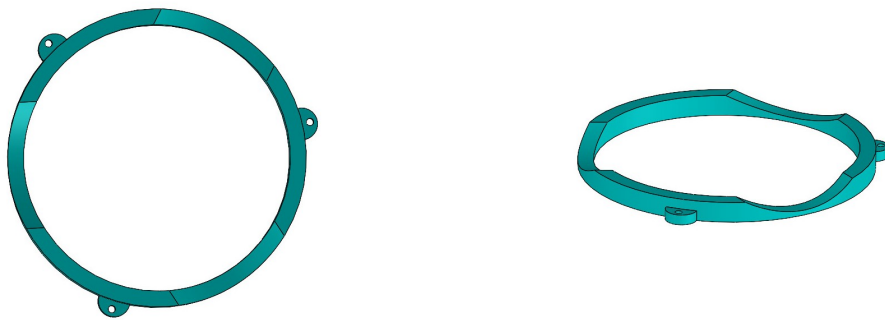


Figure 25: CAD views of the Guide Ring.

3.5 Selected Mechanisms analysis

This section provides a detailed analysis of the mechanisms selected for the payload dispenser system: the Release Arm and the Shutter. The selection of these mechanism was based on their ability to meet the stringent requirements of the mission, including reliability, simplicity, and performance in a lunar environment. This analysis will delve into the CAD models of the mechanism and the static analysis associated with them.

3.5.1 Shutter CAD models

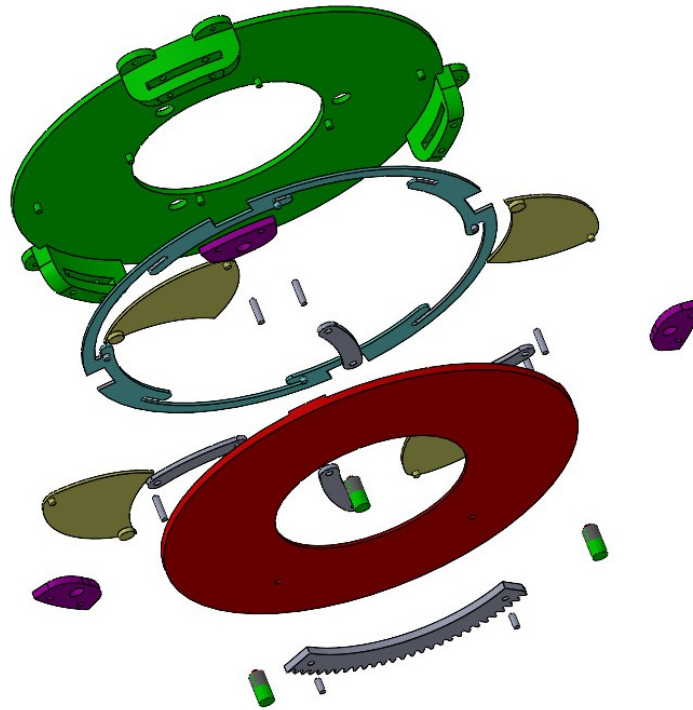


Figure 26: CAD view of the exploded Shutter.

Base

The Base has the shape of a perforated disk, with a central hole slightly larger than the radius of the spherical module containing the payloads, allowing the module to pass through smoothly. Surrounding this hole there are two circles, each composed of four pins. The inner circle is functional for the movement of the flaps: the flaps open by rotating around these pins, which serve as the center of rotation. The outer circle has been added as a safety measure to prevent the rear part of the flaps from hitting the ring that guide their movement. Essentially, these pins act as end stops for the guide slots within the guide ring. Additionally, there are three extrusions on the disk that serve to hold all the components concentric and to hold the mechanical pins in place. Finally, around the central hole, three small holes have been made to accommodate the three screws on the base plate of the system.

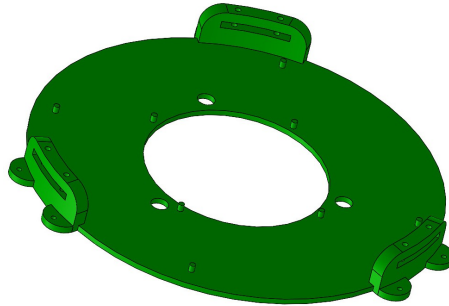


Figure 27: CAD view of the Shutter's base.

Guide Ring

This component, called Guide Ring, is necessary to push and pull the rods, thereby enabling the movement of the flaps. The ring needs to move together with the Rotating Cover (red in the figure 28). For this reason, four rectangular holes have been made on the outer part of the ring to allow it to interlock with the Rotating Cover. As mentioned in the description of the Base, there are slots that limit the movement of the ring. Finally there are pins around which the rods connected to the flaps rotate.

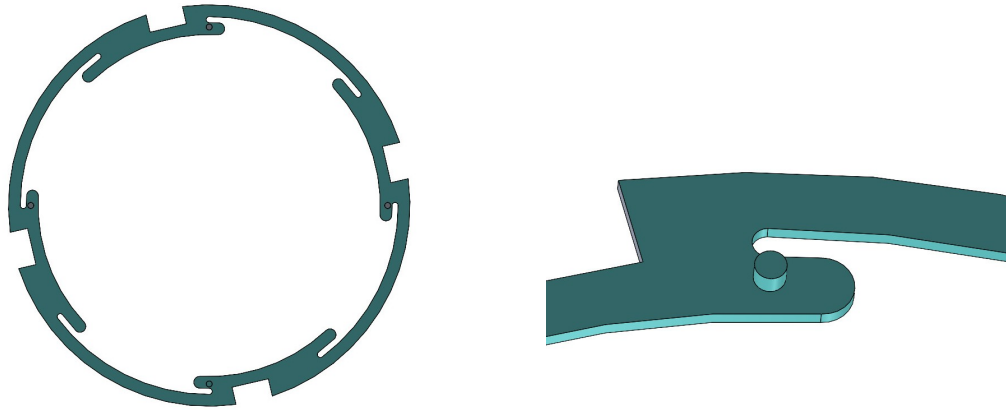


Figure 28: CAD views of the Guide Ring.

Flap

As previously mentioned in the presentation of this mechanism, the unique feature of the flaps is their shape, which allows for a perfect closure as well as a circular form when the system is open. Each Flap has a pin to which one end of the rods is connected and a hole where one of the four internal pins of the Base is inserted. Finally, there is a circular extrusion that fills the gap between the flap and the Rotating Cover maintaining the flaps stable.

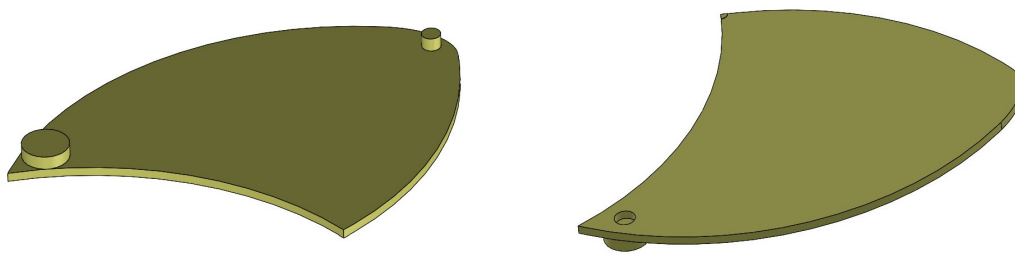


Figure 29: CAD views of a Flap.

Rod

These rods are used to link the flaps to the ring. Their arched shape facilitates movement, making the rotation of the flaps smoother.

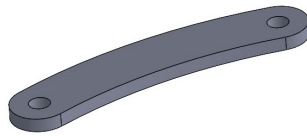


Figure 30: CAD view of a rod.

Rotating Cover

The Rotating Cover is the bottom part of the system. by rotating, this component allows the payload dispenser to open and close. There are rectangular extrusion that enable it to interlock with the Guide Ring. The central hole is the same size as the one present in the Base. Finally, there are two holes that allow the insertion of two pins to secure a gear portion in place.

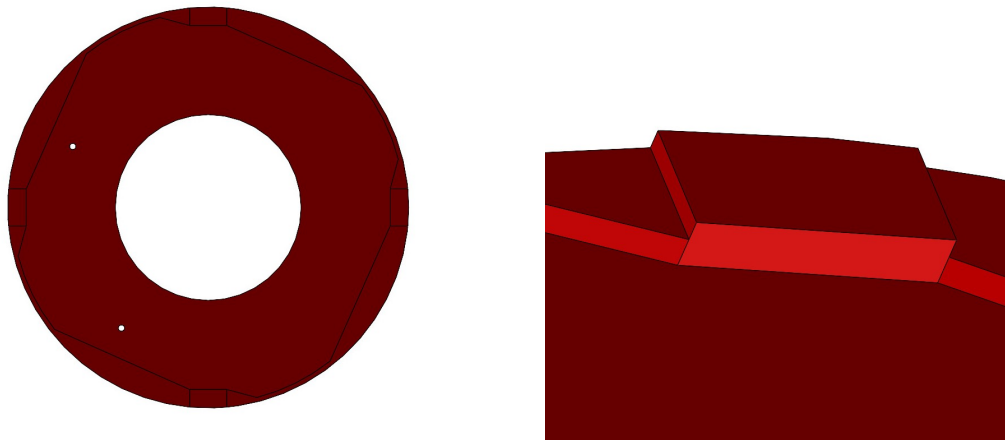


Figure 31: CAD views of the Guide Ring.

Spring Plugger's Support

This component serves to keep the Spring Plugger in place. The central hole is threaded and designed to house the Spring Plugger, while the two smaller holes allow the component to be secured to the Base using pins.

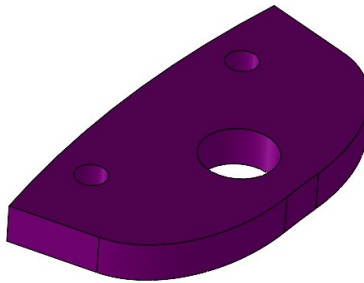


Figure 32: CAD view of a Spring Plugger's support.

Spring Plugger

This component is a Spring Plugger produced by RS PRO, it is essential for compacting the system and allowing the Rotating Cover to move. The external threading makes it ideal for screwing it into the support's hole.



Figure 33: RS PRO's Spring Plugger. [22]

3.5.2 Release Arm CAD models

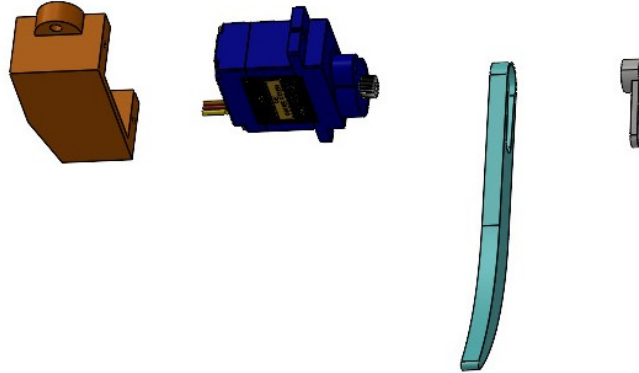


Figure 34: CAD view of the exploded Release Arm mechanism.

Actuator Arm

This component is designed to match the spherical shape of the payload module, allowing to keep it in place within the duct. At one end, there is a recessed area where the support connected to the stepper motor fits.



Figure 35: CAD view of the Actuator Arm.

Motor Support

This component is designed to house the servo motor, optimizing space building it around the shape of the motor itself. It features a cut on the lower part to allow signal and power connections between the servo and external

components. Additionally, it has two holes on the top for securing the servo to the support and two holes on one side for attaching the support to the duct as shown in figure 24.

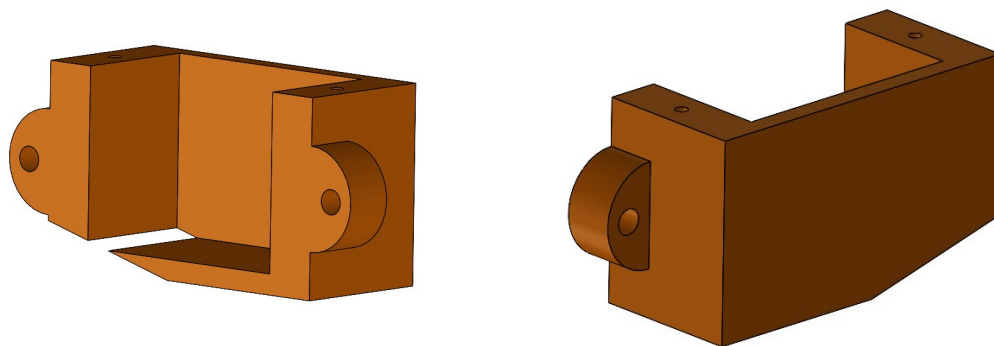


Figure 36: CAD views of the Motor Support.

In conclusion, considering only the structural components and mechanisms, the whole system, produced using the aluminium alloy A6061 has a weight equal to 5.54 Kg.

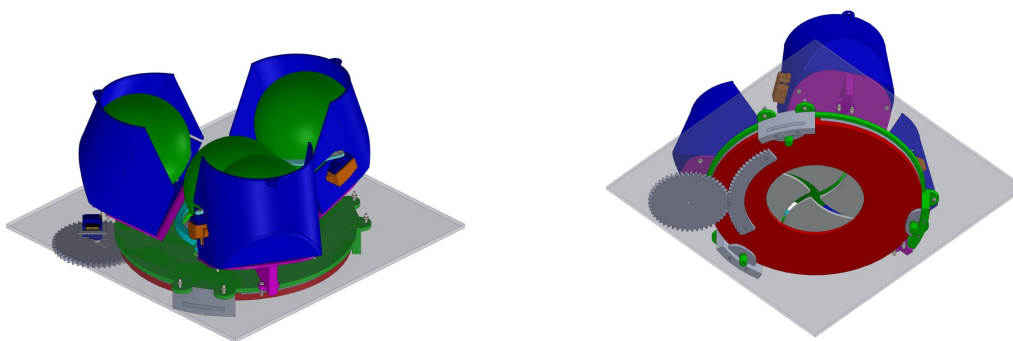


Figure 37: CAD views of the Motor Support.

3.6 Simulations and Structural Analysis

This section will present the static structural analysis of the system's critical components. The aim is to evaluate how these parts respond to static loads, focusing on areas under the highest stress. Using finite element analysis (FEA), the distribution of stress and deformation will be examined, identifying any stress concentrations and potential weak points. This method ensures that the essential components maintain structural integrity, providing reliability and strength where it is most needed.

3.6.1 Analysis of the Forces Involved

Before proceeding with the characterization of the forces, it is crucial to precisely define the arrangement of the payloads within the system, as they represent the main loads. As expected, the first three payloads are housed within the ducts. While, to optimize the transport capacity, the available space in the central part of the system has been utilized (as shown in figure 41), deciding to place a payload above the releasing port, thus maximizing the use of space. Therefore, the most critical points are the tip of each flap and the end of the actuator arm.

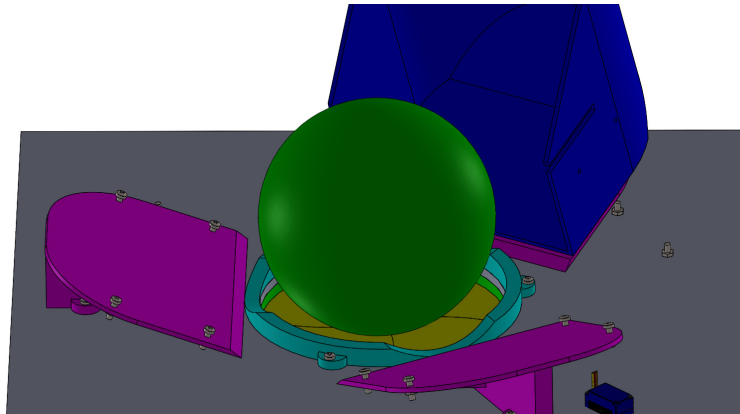


Figure 38: The placement of the fourth Payload, for simplicity two of three ducts has been removed.

Now, it is essential to carefully analyze the entire mission, from the beginning of the assembly to the arrival on the lunar surface, to determine when the system will be subjected to the highest stress. During the assembly phase, it can be assumed that the components are only subjected to Earth's gravitational acceleration of 9.81 m/s^2 . On the lunar surface, the components will experience the lunar gravitational acceleration of 1.62 m/s^2 . However, the highest acceleration will occur during the initial launch phase. Assuming the use of an Ariane 5 rocket, commonly used by ESA, the system may be subjected to acceleration up to 4.5G during the first stage of the launch. Therefore, this will be the moment when the forces on the system will be most significant.

Hence, the simulation will be carried out assuming an acceleration of 45 m/s^2 and that the forces are applied at the point cited before.

3.6.2 Simulation Results

Shutter

As mentioned earlier, an acceleration of 45 m/s^2 has been set and a force of 45 N has been applied to the central point of the release port (11.25 N applied to each tip of the flaps). This force represents the presence of a payload with a mass equal to 1 kg placed on the flaps.

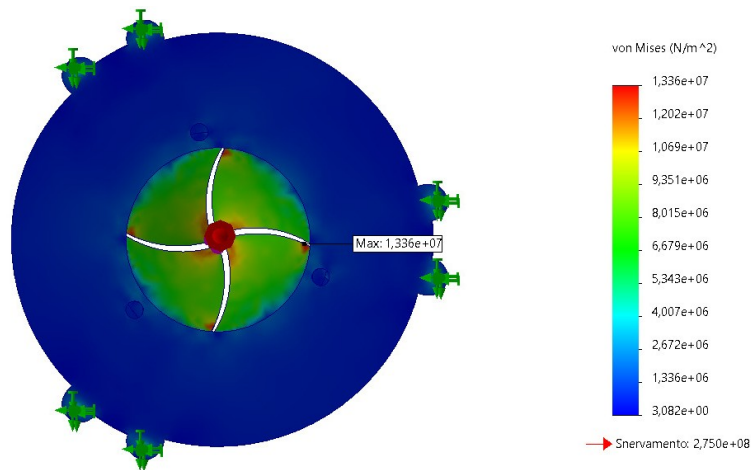


Figure 39: Shutter's yielding graph.

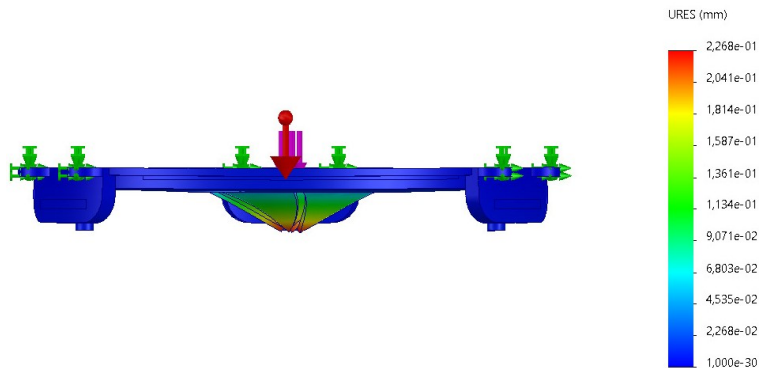


Figure 40: Shutter's displacement graph.

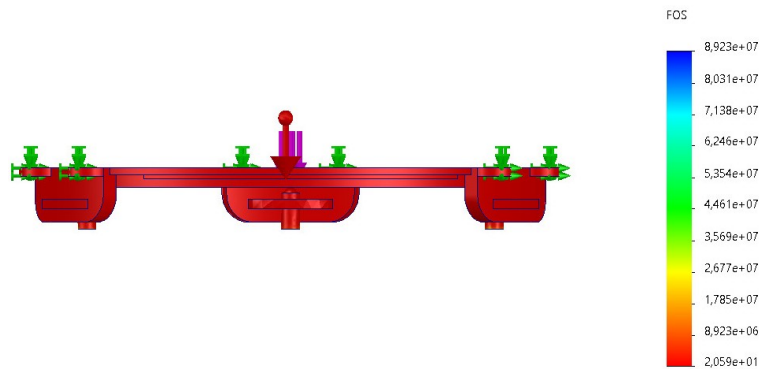


Figure 41: Shutter's coefficient of security graph.

As can be seen, the system can handle the applied loads perfectly. The Factor of security (SOF) at the most stressed point is 20.59. Even though the SOF is very high, reducing it would be counterproductive, as it would lead to an increase in displacement, which currently is in the order of tenth of millimeter, and it is preferable not exceed this value in order to keep in position the payload preventing it from getting damaged by moving inside the duct.

Release Arm

As for the Release Arm, the calculation of the force must take into account the inclination of the duct support (20°). Based on this data and considering again a system acceleration of 4.5G, a force of 14.5 N is applied to the face of the Release Arm in contact with the payload module.

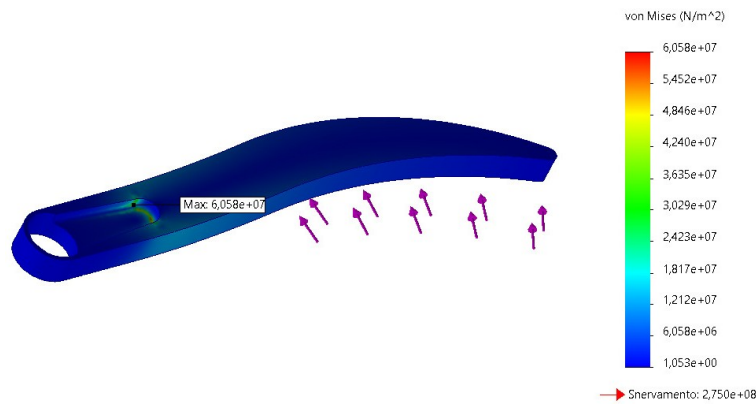


Figure 42: Shutter's yielding graph.

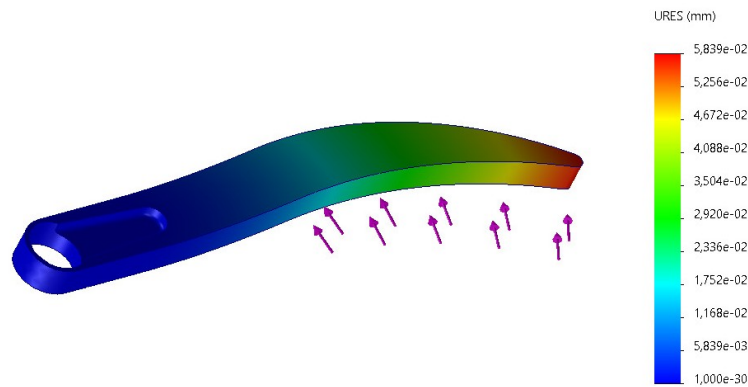


Figure 43: Shutter's displacement graph.

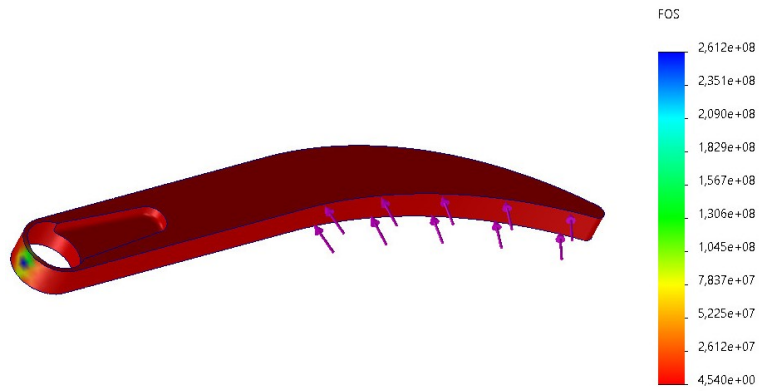


Figure 44: Shutter's coefficient of safety graph.

The results show that the Release Arm handles the applied loads well. The FOS is 4.54, while the maximum displacement is 5.84×10^{-2} mm. Both values are acceptable for the purposes of the mission.

4 Electronic and Control Design

This chapter deals with the electronic and control logic design for the payload dispenser, paying more attention to developing a simple and effective system rather than considering complications such as temperature and radiation, which would make the design complex beyond the scope and means of this project.

4.1 General Architecture

The electronic system of the payload dispenser is designed to manage the release of the different payloads on the lunar surface. To this aim several hardware and software components have been developed or integrated. In this section, the principal components used in the design of the electronic architecture and their operations in synergy are presented.

4.1.1 Integration with the Lunar Rover

Since the payload dispenser has been conceived to be integrated with several different rover systems, both power supply levels and communication protocols must be standardized and as flexible as possible. Concerning the alimentation, since servomotors have been chosen as actuators, a 5V tension is ideal for supplying the system. Furthermore, to enable communication between the microcontroller that directly manages the actuators and the central computer of the rover, microROS, a very recent development of ROS2, has been exploited

4.1.2 Rover Payload Central Computer

The central computer coordinates all the operations of the rover system, including the management of the payload dispenser's operations. For the development of the prototype, the Raspberry Pi 5 (RPi5) has been chosen, thanks to its processing power and capacity to support ROS2, it represents the ideal solution for this kind of application. RPi5, through microROS, issues commands to the dispenser's microcontroller and receives feedback from it. Thanks to its flexible architecture, the central computer can manage both the payload release operations and the system update in real-time, ensuring optimal dispenser management.

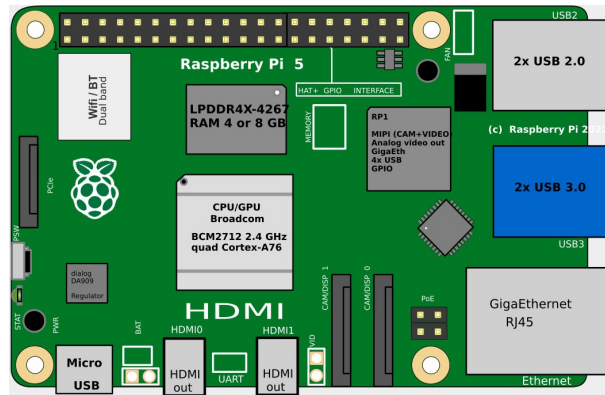


Figure 45: RPi5's schematic top view.

4.1.3 Microcontroller

The microcontroller is the core of the payload dispenser system. It serves as a direct interface between the command sent by the central computer and the actuators that physically execute the payload release. During the prototyping phase, the ESP32 DevKit V1 has been used. It is known for its high digital and analog input/output handling capability, as well as its wireless connectivity capabilities. The ESP32 is responsible for the real-time management of both the control signals from the RPi5 and those locally generated by sensors and actuators. This allows for a decentralized system where the microcontroller can operate rapid control actions such as precisely adjusting the position of actuators.

The integration of the microcontroller with the central computer has been projected to be as flexible as possible thanks to microROS. This means that, besides handling the actuator's operation, the ESP32 can be easily reprogrammed or extended to manage other components, such as sensors or other communication interfaces, making the system adaptable to different missions and operative scenarios without the need for significant hardware changes.

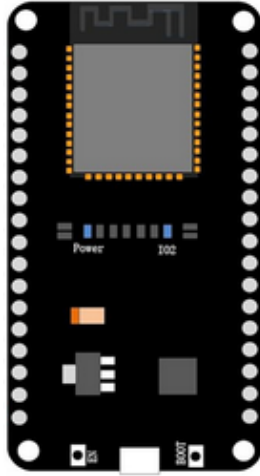


Figure 46: ESP32 DevKit V1's schematic top view.

4.1.4 Signal Decoupler

Signal decoupling is essential in every application that exploits a microcontroller to send signals to the actuators. It is in charge of separating the control signal coming from the microcontroller from those that effectively drive the actuators. This separation is crucial to avoid interferences or malfunctions caused by unwanted electrical signals protecting the microcontroller from overvoltages. The decoupler ensures that the system operates stably even under difficult conditions, such as the simultaneous release of multiple payloads.

To obtain the signal separation, a system of optocoupler has been implemented. An optocoupler is an electronic component that exploits light to transmit signals between two insulated circuits. It works thanks to an internal LED which, when the current flows in, emits light that is detected by a phototransistor located on the opposite side of the component. Then, the phototransistor activates, closing the exit circuit without a direct touch between the two circuits.

In this particular application, there are four different servomotors to be driven, hence, four different decoupling channels are required.

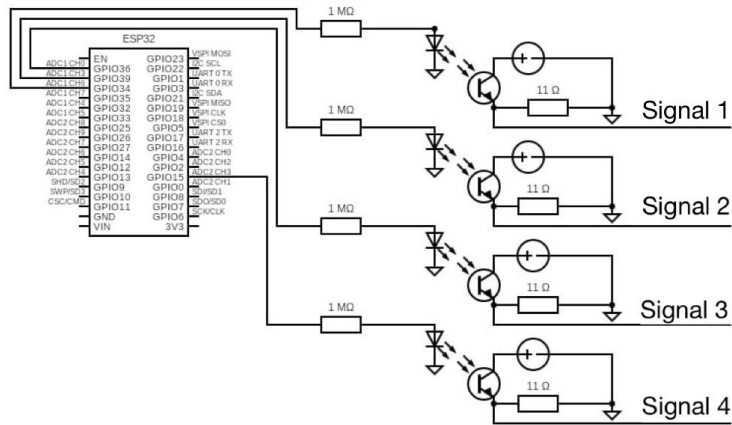


Figure 47: Decoupling circuit's schematic view.

4.1.5 Actuators

Actuators are pivotal in the development of the payload dispenser prototype. In this project, MicroServos 9g have been used. These servomotors are characterized by their small size and lightweight. They are particularly suited for applications that require controlled and precise angular movement. The standard rotation that this kind of servo offers goes from 0° to 180° making them perfect for the opening and closing movement of the shutter mechanism and the operation of the release arm.



Figure 48: MicroServo 9g.

These motors are driven by Pulse Width Modulation (PWM) signals. The duration of the pulse determines the rotation angle of the servo. This approach guarantees a smooth and precise movement, avoiding damage to the payload. In order to drive servomotors the library ESP32Servo.h has been exploited. This library makes the servomotor's control far easier since it automatically takes care of generating the PWM signals necessary for their movement.

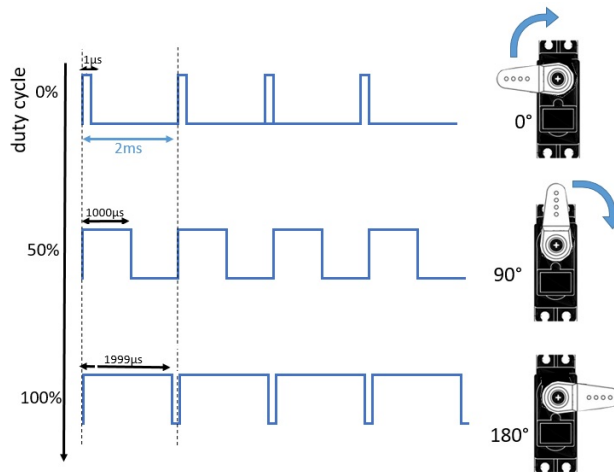


Figure 49: PWM signal and related servo position. [23]

4.2 Control Logic

The control logic for the payload dispenser has been implemented with a simple release counter. This counter drives the different servomotors based on the signals coming from the rover's central computer. The decision scheme, as represented in the diagram (figure 53), shows the process of selecting the payload to be released.

Initially, the variable `deployment_counter` is equal to 0. When the system receives a release request, this counter is increased by one. Then the hatch is opened. This is a critical step to ensure a release without mechanical obstacles. After that, the system checks the status of the counter to select the payload to release. Finally, after the release the hatch is closed to isolate the system from the lunar environment.

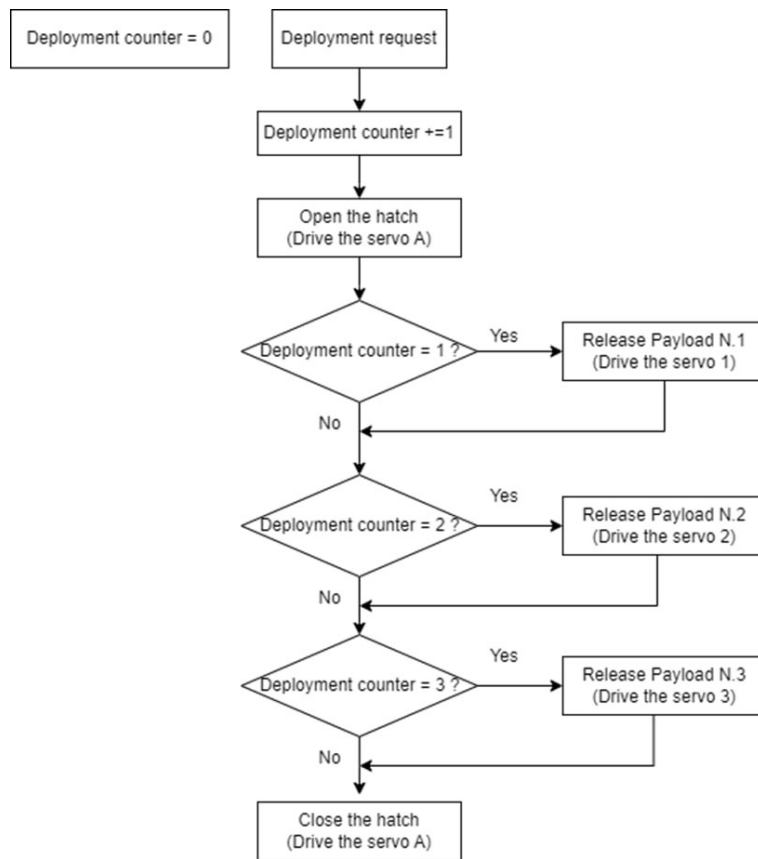


Figure 50: Control logic diagram.

In the following, there is a short description of the program running on the microcontroller that incorporates this logic.

The release command is sent by the rover central computer on the ROS2 topic `keyboard_input`. When the command is received by the microcontroller, a function called `keyboard_input_callback`, following the previously described logic manages the release sequence. This function ensures correct timing between the release moment and the shutter mechanism's opening and closing. This program also contains the different functions that manage the feedback signals. This functionality will be detailed in the next sections.

4.3 Payload Feedback Mechanism

The payload dispenser has been projected to provide feedback on the payload pose, exploiting both active and passive feedback mechanisms. This feedback mechanism is essential in order to ensure that the rover correctly knows the orientation and location of the payload after the release.

4.3.1 Active Feedback

The active feedback has been designed around an IMU sensor mounted on the payload. This sensor collects data concerning the pitch and roll parameters and then computes the payload pose. The absence of an absolute heading reference on the Moon makes it impossible to compute the yaw angle using an IMU sensor. So, this information will be acquired by exploiting another system, presented in the next section.

To estimate roll and pitch, the Madgwick Filter [24], which is a sensor fusion algorithm that combines data from the accelerometer and gyroscope to evaluate the real-time orientation has been implemented. This filter optimizes the data elaboration, reducing errors and oscillations that naturally arise when dealing with sensorial measures and ensuring an accurate pose estimation even under dynamic movement conditions or measurement instability.

The algorithm is suitable for environments with limited computational resources and when it is required to combine data from IMU sensors. This filter has been implemented on an ArduinoNanoESP32 (AN32) mounted inside the payload. The application running on the AN32 analyzes the filtered data in order to determine when the payload has stabilized and then takes the orientation to be sent to the payload dispenser microcontroller. This communication between microcontrollers has been implemented thanks to ESP-NOW, a wireless communication protocol developed by Espressid, allowing direct and low-power communication between ESP32 devices without needing Wi-Fi connectivity.

When the pose is received by the payload dispenser microcontroller, it is published on a ROS2 node `pose_communication` in order to visualize the payload frame on RVIZ2



Figure 51: Inside view of the validation payload.

Figure 54 shows the interior of the validation payload, the MPU sensor is centered inside the sphere and it is attached to the AN32. The system is powered by a 9V battery placed on the bottom of the payload.

4.3.2 Passive Feedback

The passive feedback is provided by an AprilTag printed on the payload. This tag acts as a visual reference for a cam placed on the bottom of the payload dispenser system. AprilTags allow to determine the position and orientation of the payload by exploiting artificial vision algorithms. Since all the computational processes take place on the rover's onboard computer, it is considered a passive feedback system from the payload side, it does not require alimentation.

The process to determine orientation and position starting from the AprilTag is the following:

1. **Tag detection:** The cam identifies the black edge of the AprilTag, which is designed to be easily located even in low light conditions. This allows to the algorithm to isolate the marker from the background.

2. **ID decoding:** Once the edge is identified, the algorithm analyzes the pattern within the tag, decoding it and associating the tag to a unique ID. This could be useful in the case of multiple payloads.
3. **Pose estimation:** Once the tag is identified, the algorithm is able to precisely estimate the position and orientation of the payload with respect to the camera. This is possible because the physical size of the tag placed on the payload is known in advance. The algorithm exploits this information, in combination with the captured image, to compute the distance between the cam and the tag. Thanks to the known geometry of the tag, starting from the information about the distance, it is possible to derive how the vertices of the tag are displayed in the image and so compute the position of the payload in the tridimensional space.

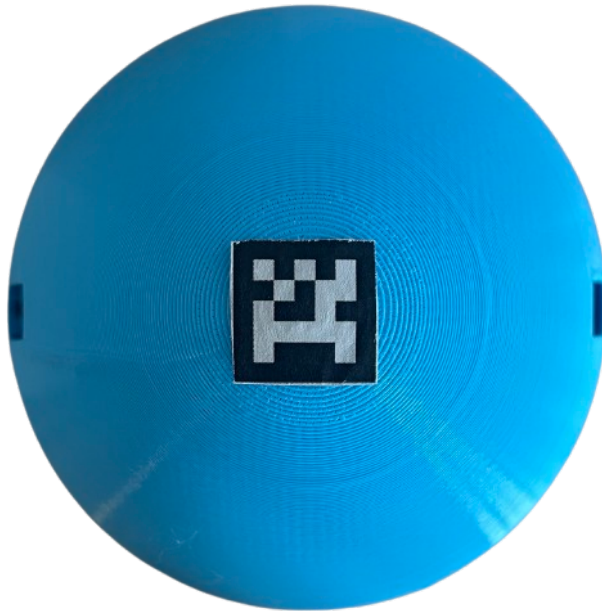


Figure 52: Top view of a payload equipped with AprilTag.

AprilTags are usually used to compute both the position and orientation of the object in the space since the algorithm can estimate also the rotation around the three axes. However, in this case, AprilTags are exploited to determine only the position and the yaw angle of the payload. This decision arises from the location of the tag on the payload which can make it difficult to precisely estimate the pitch and roll.



Figure 53: The cam, that is used for AprilTag detection, placed on the bottom of the payload dispenser.

The whole passive system feedback is managed by the RPI5 thanks to ROS2 nodes. After the estimation of the position, this information is sent to a node that merges it with the pose information in order to publish the whole pose to be shown on RVIZ2. The computed position needs to be translated in order to obtain the location of the payload with respect to the center of the system from the one computed with respect to the center of the cam.

The robust system to monitor and control payloads in complex scenarios like lunar scenarios is ensured by the combination of AprilTag-based position calculation and active feedback data provided by the MPU.

4.4 MicroROS and its integration in the project

As previously said, the communication between RPI5 and the payload dispenser's microcontroller takes place through MicroROS. MicroROS is an extension of ROS2 designed to be implemented on microcontrollers and devices with limited resources. This innovative instrument allows to exploit the potentialities of modern robotics even in scenarios where the hardware (microcontrollers in this case) cannot support the complete version of ROS2. MicroROS offers a modular architecture that is perfectly integrated with low-level control systems. [25]

4.4.1 MicroROS's Advantages

The adoption of MicroROS in this project shows the following advantages:

- **Direct execution on microcontrollers:** Thanks to its light architecture, MicroROS allows the execution of ROS2 nodes directly on microcontrollers, simplifying the communication and the actuator's control.
- **Interoperability:** MicroROS ensures fluid communication between the rover and the microcontroller, facilitating the data exchange and operation tracking. This is crucial in scenarios where the latency and affordability of communication can affect the mission result.
- **Autonomous Control:** The possibility of direct communication between complex decision-making algorithms running on the rover's central computer with low-level actuators control logic running on a microcontroller allows the autonomous management of the operation improving the reliability of the whole system.

4.4.2 MicroROS integration in the project

The integration of MicroROS in the payload dispenser project has occurred through the following steps:

- **Firmware design:** The microcontroller firmware has been developed to include a MicroROS node that manages the release operation and active feedback acquisition. This node directly communicates with the rover's central system, ensuring coordinated operations.

- MicroROS agent:** The MicroROS agent has been built into the ROS2 system on RPI5. The MicroROS agent is a pivotal node in the MicroROS environment. It manages the bidirectional communication between the RPI5 and the ESP32 microcontroller, linking the MicroROS node with the wider ROS2 system. Thanks to the MicroROS agent the payload dispenser can receive the commands coming from the rover. At the same time, always thanks to the MicroROS agent, the microcontroller can send to the rover system the feedback about the payload release.

In summary, MicroROS is a major step forward for robotics, enabling not only more reliable but also more flexible and easily reconfigurable systems.

4.5 An Overview on the Software Architecture.

In Figure 56 it is shown the RQT graph of the ROS2 environment. Every node runs on the RPI5 except for `/micro_ros_platformio_node` runs on the ESP32 and controls the release logic and receives the IMU signals from the AN32 and sends it back to the RPI5 on the topic `/pose_communication`. The node `tf_to_xyz_node` accounts for receiving the position and orientation information, merging and publishing it in order to be visualized on RVIZ2.

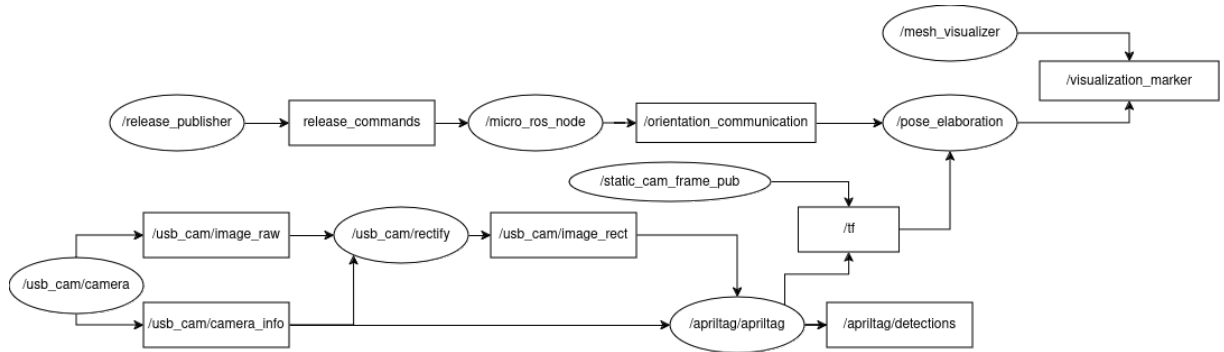


Figure 54: RQT_graph of ROS2 environment.

4.6 Components testing

Testing the electronic components is a crucial phase during the electronic system design and implementation process. It allows to verify the function-

ality, robustness, and reliability of each system element. Each component must be tested under controlled and known conditions in order to guarantee that its performances are compliant with the desired ones.

The testing phase plays an even more critical role in the context of complex systems, such as those that include microcontrollers, sensors, and actuators. A methodic approach allows to identify any possible integration issues preventing future failures or malfunctions

4.6.1 Signal Decoupler testing

Testing the decoupling circuit is pivotal in order to verify the correct transmission of the signal between the control signal sent by the ESP32 from the control side and the signal received by the microcontroller from the power side.

In order to verify the correct behavior of each decoupling channel, each optocoupler has been tested using a PWM signal in order to simulate the control signal that drives the actuators.

Test Setup:

To carry out the test the following setup has been implemented:

- **Signal Generator:** The signal generator has been set to generate a square wave with a peak-to-peak voltage of 3.3V and an offset of 1.75V. The wave period was 20 ms equal to a frequency of 50 Hz. This wave is the typical PWM signal generated by microcontrollers. The duty cycle (DC) of the signal changed for each channel tested:
 - Channel 1 DC = 10%
 - Channel 2 DC = 20%
 - Channel 3 DC = 30%
 - Channel 4 DC = 40%
- **External Power Supply:** The output channels of the optocouplers have been powered with a 5V tension with a current limitation set to 0.2 A in order to avoid overcurrents.
- **Oscilloscope:** To monitor both the input and the output signals an oscilloscope has been used

- **Circuit:** The circuit shown in Figure 50 has been implemented using a breadboard, the resistors displayed in the figure and an ILQ615 4-channel optocoupler

Resistors:

- 4x 1 $M\Omega$ resistors (Input)
- 4x 11 Ω resistors (Output)

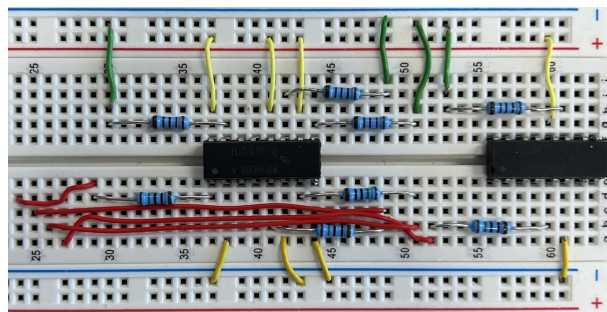
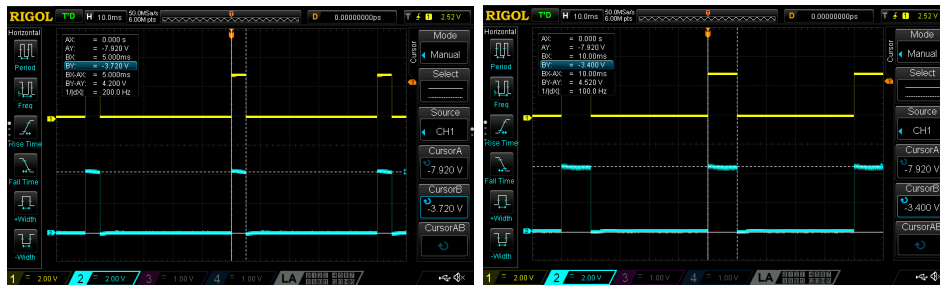


Figure 55: The Decoupling Circuit implemented on a breadboard.

Test Procedure

1. **Power Supply:** Using the power supply the optocoupler's output channels have been powered.
2. **Input Signal Generation:** The aforementioned input wave has been generated thanks to the signal generator changing the Duty Cycle depending on the channel under test to simulate different positions of the servomotors.
3. **Input/Output Monitoring:** Thanks to the oscilloscope both the input and the output signals have been visualized and analyzed to determine the correct behavior of the decoupling circuit.

Results



(a) Channel 1 10% DC

(b) Channel 2 20% DC.



(c) Channel 3 30% DC.

(d) Channel 4 40% DC.

Figure 56: Oscilloscope signal visualization. In yellow, the input waves; in light blue, the output ones.

The obtained results are coherent with the expected ones. The output signal reached a peak-to-peak voltage of about 4V instead of a nominal 5V. This discrepancy is attributable to the presence of the pulldown resistors at the output of the phototransistors.

The pulldown resistors influenced the output signal preventing it from reaching 5V, at the same time, these resistors are essential to avoid overcurrents. Although this drops, the output signals are regular and conform to the expectations for correct signal transmission. The overall behavior confirms the correct working of the circuit without interferences or relevant signal distortion.

4.6.2 AprilTag testing

This section presents the testing process of the AprilTag detection system used to determine position in three-dimensional space. Only the tag ID0 belonging to the 25h9 family has been used, changing only the dimension. Three different tags measuring 8x8cm, 5x5cm, and 2x2cm were tested, with placements in various scenarios. The results have been compared with the measured coordinates to verify the system's accuracy.

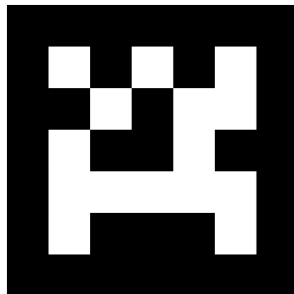


Figure 57: ID0 25h9 AprilTag.

Test Setup

To validate the AprilTag system and the correct space position evaluation, an accurate testing environment has been set up. This experimentation system has been realized to guarantee proper data acquisition and accurate evaluation.

In order to carry out the test, the following equipment has been utilized:

- **Logitech Webcam:** A Logitech webcam has been exploited in order to achieve AprilTag images. The same webcam is mounted on the bottom of the payload dispenser. This webcam has been selected because of its easy integration with ROS2 packages and its discrete resolution. The webcam has been previously calibrated in order to reduce the optical distortion
- **Laser Distance Meter:** In order to guarantee that the camera was exactly placed at the desired distance from AprilTag, a laser distance meter has been adopted. This instrument allowed to accurately measure the distance in the different experimental setups.

The webcam has been located in three different configurations with respect to the AprilTags, in order to evaluate the measure along one axes a time.

1. $\mathbf{x}, \mathbf{y} = \mathbf{0}$: varying the position on z axis
2. $\mathbf{y} = \mathbf{0}, \mathbf{z} = 40 \text{ cm}$: varying the position on x axis
3. $\mathbf{x} = \mathbf{0}, \mathbf{z} = 40 \text{ cm}$: varying the position on y axis

For each measurement, the webcam was aligned, using the laser distance meter, with a precision of millimeters. The collected data has been subsequently analyzed in order to compute the average error for each AprilTag size



Figure 58: April-Tag Distance Testing Setup.

Results

The obtained results are shown in Table 6, where are listed the real and measured values of x,y,z coordinates for each AprilTag dimension.

AprilTag Size (cm)	Coordinates (cm)					
	$x, y = 0$		$x = 0, z = 40$		$y = 0, z = 40$	
	z_{real}	z_{measured}	x_{real}	x_{measured}	y_{real}	y_{measured}
8x8	30,9	30,8	0,0	0,3	0,0	0,4
	39,4	39,7	-7,0	-7,1	-10,0	-9,5
	50,9	50,3	5,0	4,6	10,0	9,6
5x5	30,8	30,3	0,0	0,5	0,0	0,2
	40,1	40,0	-7,0	-7,2	-10,0	-10,4
	50,3	50,4	5,0	4,8	10,0	9,6
2x2	30,1	29,9	0,0	0,2	0,0	0,3
	40,0	40,0	-6,0	-5,8	-10,0	-10,1
	50,0	49,9	6,0	5,9	10,0	9,8

Table 6: AprilTag Size and Measured Coordinates.

AprilTag Size (cm)	Average error		
	z axis	x axis	y axis
8x8	0,33	0,27	0,43
5x5	0,23	0,30	0,33
2x2	0,10	0,17	0,20

Table 7: Measurement Average Error.

As can be observed from Table 7, the smaller the tag the more precise the distance evaluation. This phenomenon can be explained by different factors, the most relevant are:

- **Avoidance of error amplification:** Using smaller AprilTags the system could better evaluate the difference in coordinates with respect to greater ones, where the wider surface could amplify imprecision in angles and edges detection.

- **Optical distortion:** Larger tags (such as 8x8 cm) are more sensitive to optical distortion from the camera lens, especially at the edges of the image. If the tag is in an area where distortion is significant, the error in measurements may increase.

In conclusion, the accuracy of the system increases when smaller tags are used since they are less subjected to optical distortion and other image acquisition issues

4.6.3 MPU and Madgwick Filter testing

The objective of this testing is to evaluate the system's precision in measuring the orientation. During the test, the data obtained by the Madgwick filter are compared with the actual orientation obtained setting the roll/pitch angle of the IMU using a servo motor.

Test Setup In order to perform the tests, the IMU sensor has been attached to an oscillating plate driven by a servomotor. The plate starts oscillating and after 5 seconds the plate stabilizes adopting a determined angle. Measurements have been collected once the plate stopped moving. The measure from -40° to 40° has been analyzed for rolling and pitching, keeping one angle fixed and varying the other one.

Results

The collected data are shown in Table 8 where imposed angles are compared with the ones filtered from the sensor.

Measurement	Roll (°)	Roll measured (°)	Pitch (°)	Pitch measured (°)
1	-40	-45.6	0	-2.5
2	-30	-33.2	0	-2.6
3	-20	-20.4	0	-1.7
4	-10	-10.3	0	-1.5
5	0	0	0	0.6
6	10	10.8	0	0.6
7	20	20.5	0	0.9
8	30	31.1	0	1.5
9	40	41.5	0	1.4
10	0	0.6	-10	-13.2
11	0	0.6	-20	-23.1
12	0	0.5	-30	-34.3
13	0	0.4	-40	-44.6
14	0	0.4	0	0.3
15	0	0.4	10	12.7
16	0	0.5	30	33.4
17	0	0.5	40	44.4

Table 8: Comparison between imposed angles and measured ones.

The results indicate a proper correlation between imposed and measured angles. It can be seen when the inclination angle increases the error increases too. This behavior is shared by both roll and pitch.

Hence, the major errors have been recorded with extreme values of inclination. This attitude can be related to the quality of the sensor. In fact, MPU6065 sensors are typically used for educational purposes.

In conclusion, despite sensor limitations, tests have shown generally good behavior with errors lower than 6° in testing conditions. This suggests that the system can be used to get feedback from the released payload.

5 Realization of the Prototype

The prototype realization has represented a crucial stage in the development of the payload dispenser in order to validate the operability of the whole system. The conceptual design has been turned into a tangible and working system combining mechanical, electronic, and software components in order to test the assembled system.

5.1 Production Process

In this section, the system's production process is explained, deepening the exploited technologies, the chosen materials and the post-production phases required to obtain a working prototype.

5.1.1 3D Printing Preparation Steps

Before proceeding with the 3D printing, the CAD component files must be converted into STL files, a standard format that describes the tridimensional geometry of the objects. This phase is crucial because these files are then used by the slicing software in order to generate the G-code, that controls the printing process.

For this project, the BambuLAB A1 printer has been adopted to print most of the mechanical components. The printing setting (resolution, number of layers, supports, speed, temperatures, etc...) has been accurately defined in order to guarantee the quality and robustness required for each component.

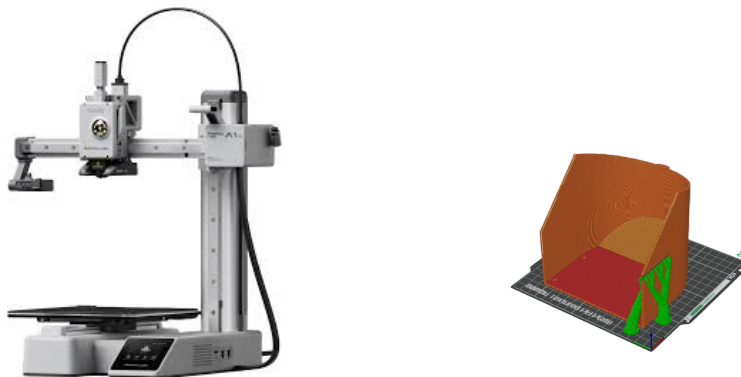


Figure 59: On the left, the BambuLAB A1 mini used to print the components. On the right, the preparation plate of the Duct.

5.1.2 3D Printed Components

Once the STL files and configured the printing settings, the components have been printed. All the mechanical printed parts of the system have been produced using PLA (Polylactic Acid), a material that offers an appreciable balance between mechanical strength and lightness. In detail, the printed components were:

- **Structure and Supports:** The main body and the support structures of the dispenser have been printed obtaining a lightweight system with a low surface finish.
- **Moving Components:** Considering the mobile components in the dispenser, these elements have been printed using 3D technologies too. In this case, however, a post-processing phase was required. Moving parts have been manually sanded to reduce friction and ensure a smooth operation. This finishing process proved fundamental to ensure a precise and functional system.



Figure 60: BambuLabA1 during the printing process of the Release Arm.

The possibility to modify and perfect the component during the post-production phases has represented a significant advantage of 3D printing, allowing to optimize of the component features without resorting to expensive traditional production techniques.

5.2 Assembly Process

After printing and post-production steps, the components have been assembled using screws, bolts and joints previously designed to facilitate assembly and ensure structural integrity. The assembling phase required particular attention to ensure that the mobile mechanism properly working smoothly and that all parts were integrated correctly allowing the system to function.



Figure 61: Disassembled Payload Dispenser.

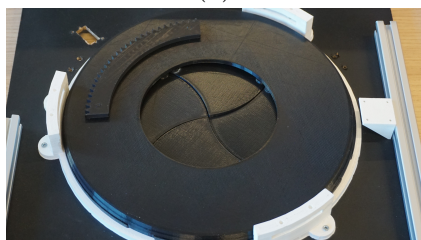
A plywood panel equipped with profiles was chosen as the basis of the system. On this panel, the Shutter's base has been fixed, and then the Guide Ring has been placed linking flaps to the ring using the rods. Finally, the Rotating Cover has been located completing the Shutter Mechanism and the mechanism has been fixed using the Spring Pluggers with their supports.



(a)



(b)



(c)



(d)

Figure 62: Figures (a) shows the Base and the Guide RIng mounted on the panel. In Figure (b) the a Rod that links the Guide Ring and a Flap. In Figure (c) the Rotating Cover. In Figure (d) the Spring Plugger.

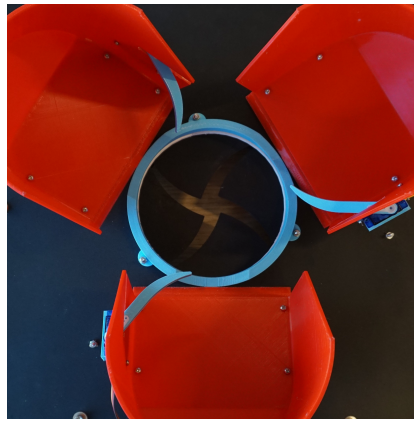
On the other side the Spacer ring has been fixed and the Ducts assembled and fixed too. Finally, the servomotors have been housed in their support fixed on the side of the ducts and the Release Arm was attached to them.



(a)



(b)



(c)

Figure 63: Figures (a) shows the Spacer Ring fixed on the panel. In Figure (b) the a Rod that links the Guide Ring and a Flap. In Figure (c) a top view of the system.

Finally, a gear has been integrated with the servomotor on the bottom of the system in order to drive the Rotating Plate.

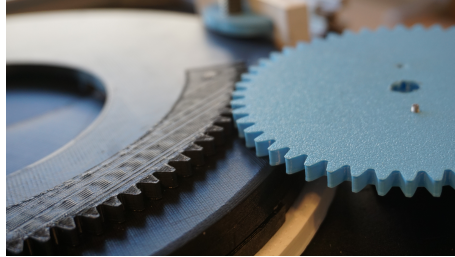


Figure 64: The mechanism that actuates the Rotating Plate.

6 Testing Phase

This chapter describes the test carried out in order to validate the functionalities of the developed system. After design and prototyping, the testing phase represents a crucial step to verify the capability of the system to operate and satisfy the design requirements. The test setup and the obtained results will be analyzed, offering a compressive evaluation of the system's performance.

6.0.1 Test Setup

Concerning the hardware setup, the test environment has been accurately projected in such a way as to allow for reproducibility. The system has been tested using a chassis made of profiles, which allows for controlled and practical testing. This configuration has made it possible to repeat tests precisely, maintaining the coherence between obtained results. The chassis offered a stable structure for mounting the payload dispenser allowing a correct evaluation of the dispenser's mechanical behavior and its integration with control electronics.

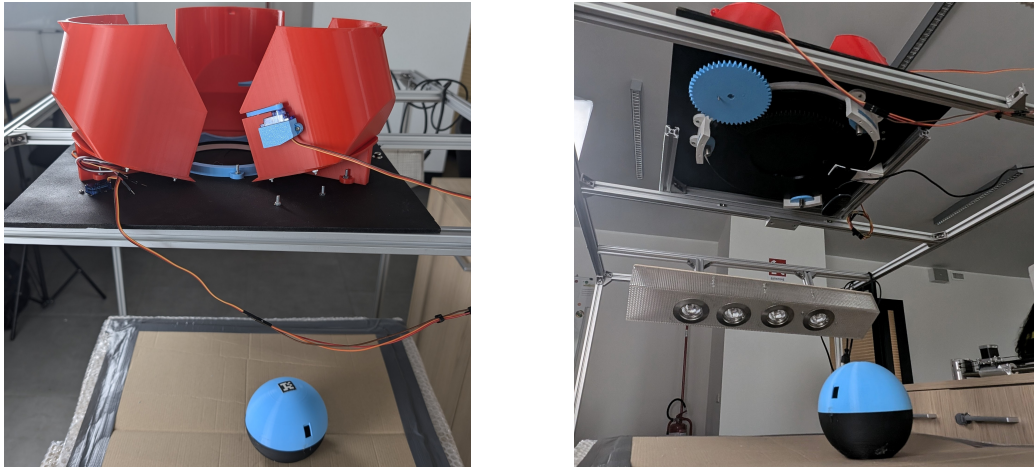


Figure 65: Payload Dispenser mounted on the testing chassis.

The distance between the chassis and the release area has been set to 40 cm in order to remain coherent with the test effectuated on the AprilTag system. The RPI5 plays the role of a central payload computer sending the release commands and elaborating the data coming from the camera and from the microcontroller.

The RPI5 was connected remotely via SSH, allowing operations to be monitored and controlled directly from a host computer. The use of SSH eliminated the need for additional physical connections between the Raspberry Pi and the control PC, making the test environment cleaner and free of unnecessary cables.

The ESP32 microcontroller carried out the task of directly controlling the payload release mechanism and executing the commands sent by the Raspberry Pi. The micro, interfaced with the servomotors and the optocoupler system, received instructions from the Raspberry Pi and managed the physical implementation of the payload release, ensuring a rapid and reliable response.

Furthermore, as anticipated in the electronic design phase, the signal has been decoupled thanks to an optocoupler system. This circuit has been supplied with 5V and a current limitation set to 0.1A. On the other side, the servo motors have been supplied with 5V too but with a maximum current set to 0.8A. Power was provided by the CPX400D a bench power supply.



Figure 66: The Payload Dispenser mounted on the chassis.

Tests have been carried out in a controlled environment, in order to avoid external interferences that could have compromised the results.

6.0.2 Test Results

The executed tests have produced very positive results, demonstrating that the projected solution satisfies widely the initial expectations. The release payload mechanism, the main object of the tests, considering the limitations due to the production process, has worked with a high rate of success. Considering 50 release attempts, the payloads were correctly released in 41 cases. Analyzing each time that the system failed a release, it was noted that the problem was due to the hatch not opening. Getting to the bottom of the problem, the hatch was blocked not due to limitations of the mechanism but due to excessive friction due to small fragments of PLA that detached from the various components of the shutter.

Furthermore, each time that the payload was correctly deployed, the communication between the ESP32 and the Raspberry Pi 5 worked successfully without any interruption. This shows the robustness and reliability of MicroROS ensuring its operability in this kind of scenario.

Considering the feedback system, both the AprilTag detection and the IMU sensor properly worked. Once the payload stabilized, the information about the pose was elaborated and sent to RVIZ2 in order to be able to visualize the position of the payload with respect to the system.

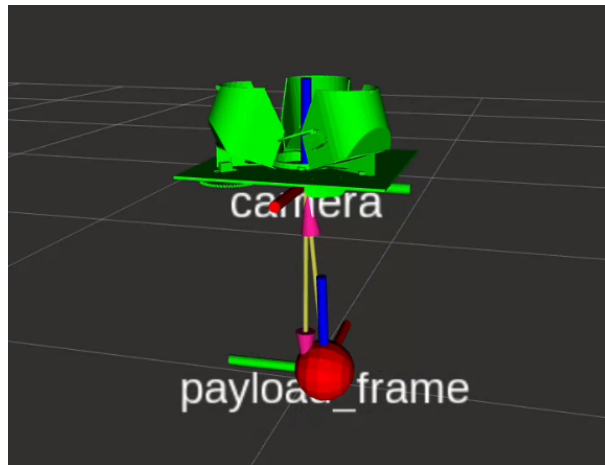


Figure 67: RVIZ2 visualization of the released payload and the system.

Finally, a crucial aspect addressed during the test was the energy efficiency. The tests have shown that the system operates with low energy consumption, confirming, as required, its fitness for long-term missions. During the idle time, the current required by the servo in order to generate a sufficient torque that keeps in position the payloads was about 0.09A. When the mechanism was activated, the servomotors required a current that peaked at 0.71A. This means, considering a fixed tension equal to 5V, that during the idle time, the system absorbed 0.45W increasing up to 3.55W in the operation period. These results are related to the aforementioned test environment and do not take into account possible increases in current that may arise from the need to apply a greater torque due to the various accelerations that come into play in the different phases of the mission.

In conclusion, the testing phase has illustrated the proper functioning of the whole system demonstrating that the payload dispenser works reliably and efficiently. The integration of the system with the AprilTag and IMU feedback proved crucial to being able to visualize the released payload even remotely without the need to visualize the operation environment. The results obtained highlight that the mechanism is ready to operate in real conditions and offers optimization opportunities for future applications.

7 Conclusion

7.1 Project summary

The project developed in this thesis focused on the development, prototyping, and validation of a payload dispenser system for a lunar exploration rover. The main goal was to design a simple and efficient system, capable of releasing different kinds of payloads while taking into account specific challenges imposed by the lunar environment. The design has been driven by modularity and flexibility concepts ensuring a straightforward integration with different kinds of rover systems. The major innovation is represented by the usage of MicroROS, a new ROS2 framework, that allows running ROS2 nodes into microcontrollers, enabling the communication between micros and a master computer.

The design phase included the development of the electronic circuit and control logic capable of ensuring accuracy and reliability during payload release. The tests were conducted both in simulations and on physical prototypes, allowing the effectiveness of the developed system to be verified and the design choices to be validated.

7.2 Summary of Achieved Results

The obtained results have shown the validity of the system, stating that it is capable of operating with efficiency, reliability and low power composition, three pivotal aspects followed during the development of the system.

The FEM analysis, conducted in simulation, has shown that a system realized in an aluminum alloy is suitable to withstand the loads that characterize an extraterrestrial exploration mission while maintaining a limited weight of the structure.

The physical tests have validated the operation of the control logic in combination with the mechanical mechanisms responsible for the payload release while also providing information about the power absorbed by the whole system.

The communication between the payload microcontroller and the rover's payload management computer, based on microROS, has proven to be efficient and stable. This aspect allowed precise and real-time control of the release operations, ensuring the receipt of numerical feedback which, once processed, allows to visualize a graphical representation of the system and the payload

with a precise relative positioning.

7.3 Contributions to Innovation of the Project

The implications of this project are considerable because the developed dispenser represents a practical and realizable solution to manage the release of payload in extraterrestrial environments avoiding the need for complex systems such as robotic arms. The implementation of MicroROS turned out crucial in order to guarantee a functional merging between high-level computational power and data elaboration and low-level actuators control. This framework offered a reliable and flexible way for communication between microcontrollers and computers.

In conclusion, the mechanical design demonstrated how a simple but robust system can be integrated into a lunar rover to accomplish delicate tasks.

This work contributes to the development of technologies for space exploration and offers potential future applications for other missions. The modularity and efficiency of the system make it easily adaptable to different contexts, expanding the possibilities of robotic exploration both in space and on Earth.

8 Future Developments

The project illustrated in this thesis project stands as a prototyping solution for the release of payloads onto the lunar surface combining efficiency, simplicity and modularity. However, as with every system in a development phase, there is plenty of room for improvement and possible future evolutions, which can improve efficiency and applicability in more complex scenarios. This chapter focuses on the potential technical improvements and the usage of this system in contexts different from the lunar explorative one.

8.1 Potential Improvements and Optimizations

8.1.1 Deployment Surface Analysis

One of the most relevant improvements concerns the development of a surface analysis algorithm. Using artificial intelligence and machine learning algorithms, it is possible to develop adaptive and intelligent analysis systems that can dynamically evaluate lunar soil conditions before releasing payloads. The adoption of this kind of algorithm can significantly improve the rover's ability to determine if the location is ideal for release. For example, the system could automatically identify stable areas for the deployment, avoiding irregular, sandy or excessively inclined surfaces, which could compromise the integrity of the payload.

Beyond the deployment location selection, the system could even contribute to optimize the payload positioning. For instance, once the release site has been determined, the algorithm could compute the ideal payload pose in order to maximize the efficiency and stability according to the surface conditions.

8.1.2 Material Improvements

Another crucial optimization field regards the improvement of the material used for the system realization. In this prototyping step, the PLA has been used to obtain a first model of the mechanisms. The next evolution of this project could include the realization of some components in aerospace materials such as aluminum alloys, composite materials or materials that exploit nanotechnologies, this will optimize the weight-strength properties of the whole system making another step to the final mission-level system. Beyond that, insulating materials can be adopted in order to evaluate the thermal

property of the system in lunar environment test conditions. In this context, Aerogel can be a solution to isolate the system from the external environment. In fact, this material has been already used by NASA in the realization of the Mars Exploration Rover.

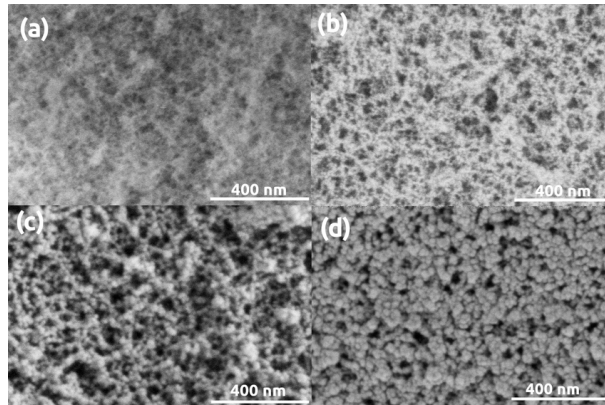


Figure 68: Low Voltage Scanning Electron Microscopy (LVSEM) images of silica aerogel samples. (a) Pristine, uncoated. (b-d) Sputter coated with 5 nm, 16 nm, 32 nm thick Au layers, respectively. [26]

8.1.3 Release Mechanism

A further potential improvement is represented by the optimization of the payload release mechanism. The current design, even if is simple and functional, could be perfected by the introduction release mechanism with an elevated resilience to environmental variations.

A possible approach is depicted by the adoption of a magnetic actuation systems, which are capable of operating with precision, lowering energy consumption.

Furthermore, a feedback system that evaluates the correct opening of the shutter can be implemented in order to avoid payload damage during the release. For example, piezoelectric sensors could be placed to ensure the correct position of each flap during the opening phase. Only after all the sensors confirm that each flap has reached the end of its path will the release be allowed.

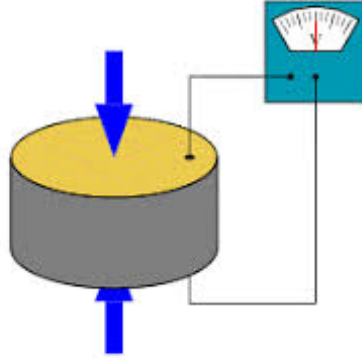


Figure 69: Piezoelectric schematic working principle. [27]

8.2 Applicability in Other Contexts

8.2.1 Celestial Bodies Exploration

Even if the system has been projected to operate principally in a lunar exploration context, its modularity characteristics favor adaptability in a wide range of different scenarios, both in spacial and terrestrial environments. In the first place, the system could be adapted for exploration missions on several celestial bodies, such as Mars, asteroids or other planet moons. In this context, the technical and environmental challenges are similar to the ones faced during this thesis project with the addition of new variables, such as thin atmospheres or even more extreme temperatures. The system, projected in the most generalizable way, can be easily modified to face these conditions, for example, by improving the thermal protections.

8.2.2 Support for Extravehicular Missions

Another interesting application field is represented by the support of astronauts during extravehicular missions. In this context, the system can be integrated outside space structures such as spacecraft or stations in order to supply items, equipment and other useful resources to conduct extravehicular missions such as maintenance. In this case, an additional implementation mechanism would be required to eject objects if centrifugal force is not present either.

8.2.3 Exploration of Extreme Terrestrial Environments

Another application scenario regards the exploration of terrestrial extreme areas. These environments, such as deserts, polar regions, and oceans, show challenges similar to those encountered during the analysis of the lunar surface. The ability to operate in extreme conditions, with limited resources and high variability of ground conditions, makes the system particularly suitable for land missions in difficult-to-access places.

8.2.4 Urban deliveries

Furthermore, the adoption of the system in the field of automated urban delivery, for example via drones, represents another possible development. With the growing demand for fast and efficient delivery systems in complex urban environments, the ability to autonomously manage the delivery of specific packages or loads would represent a significant competitive advantage. The system could easily be adapted to allow drones to load and drop packages at specific locations, reducing the need for human intervention and increasing operational efficiency.

In conclusion, the system proves to be highly adaptable and capable of evolving for the most complex applications. Several potential improvements, such as the implementation of surface analysis algorithms, the use of advanced materials and the optimization of the release mechanism, continue the path towards future research and technical improvements. These innovations could further improve the system's reliability and performance in harsh environments, improving its functionality for exploration on various celestial bodies or even in extreme terrestrial environments. Moreover, the adaptability of the system allows to use the payload dispenser for a wide range of applications spanning from the celestial bodies exploration to the urban deliveries.

9 Appendix

9.1 Guide to MicroRos Usage

9.1.1 Prerequisites

ROS MicroRos is a version of ROS2 designed to be used on microcontrollers. Its aim is to bring ROS capabilities to systems with a limited processing power, memory and storage. Since MicroRos allows the communication between ROS networks and embedded systems, a basic knowledge about ROS/ROS2 is required. In this document, it is assumed that a ROS2 distro is already installed on the computer.

Required HW/SW

- Microcontroller (MC) (in this case, an ESP32 MC will be used)
- USB-MicroUSB cable

SW

- Visual Studio Code (VSCoDe)
- Integrated Development Environment extension for VSCoDe (in this case, PlatformIO)
- MicroRos agent
- MicroRos application

9.1.2 PlatformIO Setup

VSCoDe Open the terminal and write the following line:

```
sudo apt install code --classic
```

Once the installation has ended, open VSCoDe by writing:

```
code .
```

PlatformIO extension

When VSCoDe opened, go to the top left bar and open "Extensions"



Figure 70: Extensions submenu

Search for PlatformIO extension and install it.

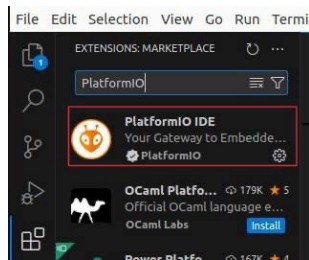


Figure 71: PlatfotmIO installation

PlatformIO new project Once installed, the submenu will appear on the left of the VSCode window:



Figure 72: PlatformIO submenu

Click on it, select *Create New Project* and then, *+ New Project*. Now, name your project, select your board and the framework. After that, deselect the option *Use default location* and choose your ROS2 workspace. This is an example of configuration:

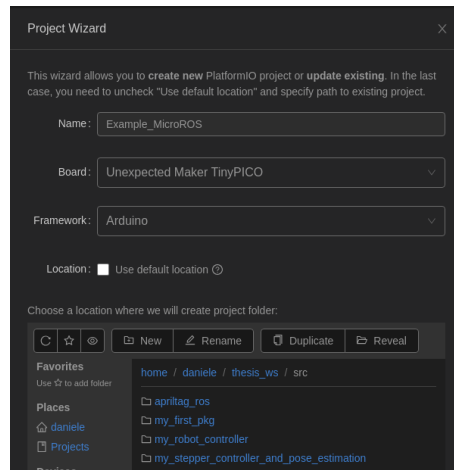


Figure 73: PlatformIO project configuration

The two most important files are `main.cpp` (the application file) and `platformio.ini` (the configuration file). Now, open the main file inside the directory `/path/to/your/workspace/Example_MicroROS/src`. The aim of this example is to run a simple publisher on the MC. To achieve this, we can copy the publisher example from [Here](#) into `main.cpp`.

After that, the file `platformio.ini` must be configured. The field `platform`, `board` and `framework` are configured by default. The library dependencies must be added. In this case, only `micro_ros_platformio` library must be included:

https://github.com/micro-ROS/micro_ros_platformio

Moreover, the type of transport must be chosen. In this case, the serial transport is used. The file must look like this:

```

Example_MicroROS > platformio.ini
1 ; PlatformIO Project Configuration File
2 ;
3 ; Build options: build flags, source filter
4 ; Upload options: custom upload port, speed and extra flags
5 ; Library options: dependencies, extra library storages
6 ; Advanced options: extra scripting
7 ;
8 ; Please visit documentation for the other options and examples
9 ; https://docs.platformio.org/page/projectconf.html
10
11 [env:tinypico]
12 platform = espressif32
13 board = tinypico
14 framework = arduino
15 board_microros_transport = serial
16 lib_deps =
17 | https://github.com/micro-ROS/micro_ros_platformio
18

```

Figure 74: Platformio.ini file

Pay attention, in this case, ROS2 iron is being used, that is the default distro for MicroRos. In case of using another distro, the following line must be included inside the `Platformio.ini` file:

`board_microros_distro = < your_distro >`

Then, save the file and wait for the update of metadata. Once the metadata are updated, the application is ready to be flashed onto the MC. Using the USB-microUSB cable, connect the board to the computer. Now, compile the file using the bottom-left menu.



Figure 75: Compilation button

If the compilation went well, the output should look like this:

```
esptool.py v4.5.1
Creating esp32 image...
Merged 2 ELF sections
Successfully created esp32 image.
===== [SUCCESS] Took 6.70 seconds =====
Terminal will be reused by tasks, press any key to close it.
```

Figure 76: Correct compilation output

Finally, upload the application onto the board using the button on the lower left menu.



Figure 77: Upload button

The obtained output should look like this:

```
writing at 0x000344eb... (46 %)
writing at 0x000399df... (53 %)
writing at 0x000404d9... (61 %)
writing at 0x00046888... (69 %)
writing at 0x00050db1... (76 %)
writing at 0x00050b6a... (84 %)
writing at 0x0005e52b... (92 %)
writing at 0x00063c8b... (100 %)
Wrote 349408 bytes (200928 compressed) at 0x00010000 in 4.8 seconds (effective 576.8 kbit/s)...
Hash of data verified.
Leaving...
Hard resetting via RTS pin...
===== [SUCCESS] Took 10.56 seconds =====
Terminal will be reused by tasks, press any key to close it.
```

Figure 78: Correct upload output

If this type of error is encountered:



Figure 79: Common error

Type the following line on the terminal to ensure that the user is in the dialout group and try to upload again the application (reboot the system before uploading):

```
sudo usermod -aG dialout $USER
```

9.1.3 MicroROS agent

MicroROS installation Once the application has been uploaded, the microROS build system must be installed.

- Create a workspace for microROS and download the MicroRos tools

```
source /opt/ros/$ROS_DISTRO/setup.bash
mkdir microros_ws
cd microros_ws
git clone -b $ROS_DISTRO https://github.com/micro-ROS/micro_ros_setup.git
src/micro_ros_setup
```
- Update the dependencies

```
sudo apt update && rosdep update
rosdep install --from-paths src --ignore-src -y
```
- Install pip

```
sudo apt-get install python3-pip
```
- Build and source MicroROS tools

```
colcon build
source install/local_setup.bash
```

MicroROS agent run Now, the microROS agent must be created. To do this, follow the next steps:

- Download the package

```
ros2 run micro_ros_setup create_agent_ws.sh
```

- Build the package

```
ros2 run micro_ros_setup build_agent.sh
```

```
source install/local_setup.bash
```

- Find the serial device name

```
ls /dev/serial/by-id/
```

- Run the agent

```
ros2 run micro_ros_agent micro_ros_agent serial --dev [device]
```

(In this case the serial name is :

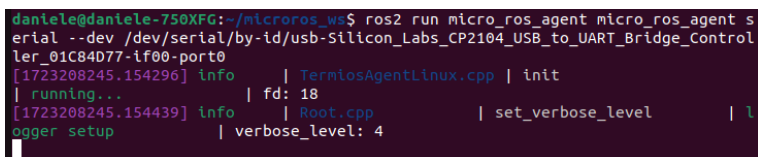
```
/dev/serial/by-id/usb-Silicon_Labs_CP2104_USB_to_UART_Bridge_Controller_01C84D77-if00-port0
```

so the command becomes :

```
ros2 run micro_ros_agent micro_ros_agent serial --dev /dev/serial/by-id/usb-Silicon_Labs
```

```
_CP2104_USB_to_UART_Bridge_Controller_01C84D77-if00-port0)
```

After that, you will obtain something like this:



```
danielegdaniele-750XFG:~/micro_ros_ws$ ros2 run micro_ros_agent micro_ros_agent serial --dev /dev/serial/by-id/usb-Silicon_Labs_CP2104_USB_to_UART_Bridge_Controller_01C84D77-if00-port0
[1723208245.154296] info | TermiosAgentLinux.cpp | init
| running... | fd: 18
[1723208245.154439] info | Root.cpp | set_verbose_level | 1
ogger setup | verbose_level: 4
```

Figure 80: Agent starting output

At this point, remove and insert USB cable of MC again and the agent has been created:

```
[1723208269.463897] info | TermiosAgentLinux.cpp | init
| running... | fd: 18
[1723208271.664216] info | Root.cpp | create_client | c
reate | client_key: 0x0E86C4A7, session_id: 0x81
[1723208271.664298] info | SessionManager.hpp | establish_session | s
ession established | client_key: 0x0E86C4A7, address: 0
[1723208271.693246] info | ProxyClient.cpp | create_participant | p
articipant created | client_key: 0x0E86C4A7, participant_id: 0x000(1)
[1723208271.709909] info | ProxyClient.cpp | create_topic | t
opic created | client_key: 0x0E86C4A7, topic_id: 0x000(2), participant_
id: 0x000(1)
[1723208271.719583] info | ProxyClient.cpp | create_publisher | p
ublisher created | client_key: 0x0E86C4A7, publisher_id: 0x000(3), particip
ant_id: 0x000(1)
[1723208271.730415] info | ProxyClient.cpp | create_datawriter | d
atawriter created | client_key: 0x0E86C4A7, datawriter_id: 0x000(5), publish
er_id: 0x000(3)
```

Figure 81: Agent final output

And this is what the node is publishing:

```
daniele@daniele-750XFG:~/microros_ws$ ros2 topic list
/micro_ros_platformio_node_publisher
/parameter_events
/rosout
daniele@daniele-750XFG:~/microros_ws$ ros2 topic echo /micro_ros_platformio_node
_publisher
data: 424
---
data: 425
---
data: 426
---
data: 427
---
data: 428
---
data: 429
---
data: 430
---
data: 431
---
data: 432
---
data: 433
---
data: 434
---
```

Figure 82: Application output

References

- [1] NASA/JPL-Caltech. *Cassini will pass through unexplored areas between the planet Saturn and its rings*. https://www.esa.int/ESA_Multimedia/Images/2017/04/Cassini_will_pass_through_unexplored_areas_between_the_planet_Saturn_and_its_rings.
- [2] ESA/ATG medialab. *Philae touchdown*. https://www.esa.int/ESA_Multimedia/Images/2017/04/Cassini_will_pass_through_unexplored_areas_between_the_planet_Saturn_and_its_rings.
- [3] NASA. *Europa Clipper Instruments*. Accessed: 2024-08-27. 2024. URL: <https://europa.nasa.gov/spacecraft/instruments/>.
- [4] NASA/JPL/DLR. *Natural and False Color Views of Europa*. Accessed: 2024-08-27. 2019. URL: <https://europa.nasa.gov/resources/91/natural-and-false-color-views-of-europa/?category=images>.
- [5] NASA. *MSL Curiosity Rover*. Accessed: 2024-08-22. URL: <https://science.nasa.gov/mission/msl-curiosity/>.
- [6] NASA/JPL-Caltech. *Mars Curiosity Rover Selfie*. 2018. URL: <https://mars.nasa.gov/resources/22046/mars-curiosity-rover-selfie-june-2018/>.
- [7] Joshua W Ehrlich et al. “Exploring extreme lunar environments through in-flight swarm deployments”. In: *2021 IEEE Aerospace Conference (50100)*. IEEE. 2021, pp. 1–9.
- [8] Rashid Ali et al. “Tightly coupling fusion of UWB ranging and IMU pedestrian dead reckoning for indoor localization”. In: *IEEE Access* 9 (2021), pp. 164206–164222.
- [9] Michelangelo Levati. “Prototyping of Energetically-Autonomous UWB Anchors for Rover Localization in Lunar Environment”. Master’s Thesis. Torino, Italy: Politecnico di Torino, 2022.
- [10] NASA. *CubeSats Overview*. Accessed: 2024-08-27. 2024. URL: <https://www.nasa.gov/kennedy/launch-services-program/cubesat-launch-initiative/>.
- [11] Ryan Hevner. “Lessons learned flight validating an innovative Canisterized Satellite Dispenser”. In: *2014 IEEE Aerospace Conference*. IEEE. 2014, pp. 1–7.

- [12] William Doggett et al. “A Versatile Lifting Device for Lunar Surface Payload Handling, Inspection & Regolith Transport Operations”. In: *AIP Conference Proceedings*. Vol. 969. 1. American Institute of Physics. 2008, pp. 792–808.
- [13] Craig Beckfield et al. *Lunar Payload Deployment System (LPDS)*. Prepared as part of the NASA Artemis Program. Lockheed Martin.
- [14] Narek Pezeshkian et al. “Automatic payload deployment system”. In: *Unmanned Systems Technology XII*. Vol. 7692. SPIE. 2010, pp. 238–249.
- [15] Lorenzo Premoli. *Cratere Plato e Sinus Iridum*. Accessed: 24-August-2024. 2021. URL: https://commons.wikimedia.org/wiki/File:Crateri_Lunari.jpg.
- [16] National Oceanic and Atmospheric Administration (NOAA). *Moon: Surface Temperature*. Accessed: 25-August-2024. 2013. URL: <https://sos.noaa.gov/catalog/datasets/moon-surface-temperature/>.
- [17] Sarah Noble. “The lunar regolith”. In: *Lunar Regolith Simulant Workshop*. MSFC-2221. 2009.
- [18] Sang H Choi et al. “Electrostatic power generation from negatively charged, simulated lunar regolith”. In: *AIAA SPACE 2010 Conference and Exposition*. NF1676L-10076. 2010.
- [19] Hao Sun et al. “Measuring adhesion of microparticles in lunar regolith simulant BHL1000 by centrifugal technique”. In: *Planetary and Space Science* 220 (2022), p. 105535.
- [20] Debay Chiamonti, National Institute of Standards, and Technology (NIST). *Moon Dust Micrographs*. Micrographs of moon dust particles collected during the Apollo 11 mission. Images were taken with a scanning electron microscope at NIST. Accessed: 25-August-2024. URL: <https://www.nist.gov/>.
- [21] Aalco Metals Ltd. *Aluminium Alloy 6061 - T6 Extrusions*. Datasheet Updated: 13 November 2018. Parkway House, Unit 6 Parkway Industrial Estate, Wednesbury WS10 7WP: Aalco Metals Ltd, 2018. URL: <https://www.aalco.co.uk>.
- [22] RS PRO. *RS PRO M10 Spring Plunger, 21mm Long*. 2024. URL: <https://export.rsdelivers.com/product/rs-pro/rs-pro-m10-spring-plunger-21mm-long/0478573>.

- [23] Meccanismo Complesso. *Arduino - Servo Motors: How They Work and How to Control Them*. <https://www.meccanismocomplesso.org/en/arduino-servo-motors-how-they-work-and-how-to-control-them/>. 2020.
- [24] AHRS Documentation. *Madgwick Orientation Filter*. 2024. URL: <https://ahrs.readthedocs.io/en/latest/filters/madgwick.html>.
- [25] micro-ROS Team. *micro-ROS: ROS 2 for Microcontrollers*. <https://micro.ros.org/>. Accessed: 2024-10-14. 2024.
- [26] Laura Juhász et al. “False morphology of aerogels caused by gold coating for SEM imaging”. In: *Polymers* 13.4 (2021), p. 588.
- [27] Wikipedia contributors. *Piezoelectric sensor – Wikipedia, The Free Encyclopedia*. 2024. URL: https://en.wikipedia.org/wiki/Piezoelectric_sensor.